Journal of Materials Chemistry A

Accepted Manuscript

ROYAL SOCIETY OF CHEMISTRY

www.rsc.org/materialsA

A Review on Recent Progress, Challenges and Perspective of Layered Double Hydroxides as Promising Photocatalysts

Lagnamayee Mohapatra [*] [a] and K. M. Parida [**] [b]

[a] Centre for Advanced Materials, Qatar University, P.O. Box 2713, Doha, Qatar

[b] Centre for Nano Science and Nano Technology, ITER, Siksha 'O'Anusandhan University Bhubaneswar-751 030, Odisha (India)

*Lagnamayee Mohapatra, Centre for Advanced Materials, Qatar University,Doha, Qatar

E-mail:mlagnamayee@gmail.com, lmohapatra@qu.edu.qa

**K.M. Parida, Siksha 'O' Anusandhan University, Bhubaneswar-751 030, Odisha, India

E-mail: paridakulamani@yahoo.com, kulamaniparida@soauniversity.ac.in

ABSTRACT

Considering the previous work on layered double hydroxides (LDHs) as novel photocatalyst, research on this group of materials has become one of the most exciting subjects of today. LDH has become an important class of layered materials having perspectives for photocatalysis, wherein a great attention has been paid to the exhaustive aerobic degradation of pollutants, photocatalytic water splitting, and CO_2 photo-reduction. The unique structure, uniform distribution of different metal cations in the brucite layer, surface hydroxyl groups, flexible tunability, intercalated anions with interlayer spaces, swelling properties, oxo-bridged linkage, and high chemical stability are some of the important advantages of this group of materials. This article provides an up-to-date review on significant progress in the fabrication of the LDH photocatalytic systems aiming at environmental clean-up and energy production, such as degradation of pollutants photocatalytic H_2 generation and photocatalytic CO_2-reduction.This article, after discussing recent significant progress in the synthesis of different photoactive LDH materials and photocatalytic applications through their structural and electronic properties, considers many typical examples. In particular, the recent progress on the emerging strategies of LDH to improve their photocatalytic activity is also presented. Eventually, the future challenges and outlooks of this group of materials are also discussed.

List of contents:

1. Introduction

Synthetic inorganic layered materials, such as layered perovskite and cationic and anionic clays with well-defined structures and tailor-made functionalities, provide special characteristics for the solution of today's environmental and clean energy problems. In this review article, considerable research efforts have been put into the design and study of different layered double hydroxides (LDHs) for photocatalysis. LDHs, generally also called anionic clays, are known as host–guest layered materials.[1, 2] However, contrary to cationic clays, LDH materials are quite rare in nature. Most of the LDHs are synthetic materials and their structures appear as the naturally arising mineral hydrotalcite $[Mg_6Al_2(OH)_{16}]CO_3{\cdot}4H_2O$, which was discovered in 1842 and first prepared as a synthetic material in 1942 by Feitknecht.[3,4] However, the detailed structural characteristics of LDHs were delineated during the late 1960s by Allmann,[5] Taylor[6] and their co-workers. LDHs are an important class of layered materials receiving a great attention in important areas such as adsorbent, catalysis, photocatalysis, photochemistry, electrochemistry, biomedical science, magnetisation, polymerisation and environmental applications.[7–12] Recently, LDH have emerged as a ground-breaking photocatalyst group in the field of energy and environment because of their several exceptional properties. The fabrication of visible active layered double hydroxide photocatalysts is currently a subject of particular importance because of their significance in both fundamental research and practical applications. Though different groups have been reported regarding neat LDHs and modified LDHs in photocatalytic degradation of organic pollutants and decomposition of water into hydrogen and

oxygen, designing a novel visible active LDH photocatalyst for industrial application is still a great challenge.

Although there have been a few reviews on preparation, properties and catalytic applications of LDH-based materials[12,13] and LDH nanosheets,[14] a strategic update is highly desirable to inform the latest progress, growing trends and updated summary of the current status with regard to photocatalysis. Although a number of research groups, particularly that of Li and co-worker have performed a lot of works in this field and summarised the use of LDH materials in the field of different heterogeneous catalytic applications. [15-16] However, the rapid growth of the use of LDH catalysts in the photocatalytical applications is requiring a fresh assessment. Therefore, the recent review aims at providing an overview of the progress of the present research in the synthesis of photoactive LDHs with various modification strategies for various photocatalytic applications. Such progress is also expected to offer an additional opportunity regarding the design and development of layered materials based photocatalysts. Layered double hydroxide (LDH)-based photocatalysts have emerged as one of the most promising candidates to replace TiO_2 –based photocatalysts for photocatalysis owing to their unique layered structure, compositional flexibility, low manufacturing cost and ease of synthesis. It compiles their unique structural and electronic properties and the information available on the special characteristics of LDHs responsible for the photocatalytic activity towards energy and environmental applications. Moreover, the fundamental strategies are discussed, which are required to enhance the photocatalytic activity. Our findings also suggest that the use of solar energy for photocatalytic water splitting for hydrogen evolution might provide a feasible source for 'clean' hydrogen fuel, degradation of organic pollutants and reduction of greenhouse gases. Furthermore, this review attempts to demonstrate the well-established mechanism and use of the LDH photocatalyst for

photocatalytic reactions. We hope this review will benefit the interested researchers in the field of photocatalysis by layered materials.

2. Synthesis of Photoactive LDHs

In the past few years, several studies related to the synthesis of LDH materials have been rapidly published. They discuss simple and inexpensive methods to synthesise both in laboratory and at an industrial scale. Many methods allowed the preparation of materials with tailored physical and chemical properties suitable for many applications. [17-19] As there have been several review articles towards the preparative chemistry of LDH materials, herein our focus is primarily on the synthetic methods closely associated with photoactive LDHs.

2.1. Co-precipitation method

In the pioneering work on the LDH as a photocatalyst, co-precipitation is the most common preparative method followed by the researchers. For the first time, Garcia et al. reported a simple co-precipitation method to synthesise Zn–Cr, with NaOH and urea solution as precipitators for photocatalytic applications.[20] It was based on the slow addition of the mixed solution of divalent and trivalent metal salts in an appropriate ratio and a second (alkaline) solution to the reactor containing water. The simultaneous addition of mixed metal salts and alkali maintains the pH at a selected level, leading to the co-precipitation of the two metallic salts. The mechanism of co-precipitation is ideally based on the condensation of hexa-aqua metal complexes in solution, leading to the formation of the brucite-like layers with close to evenly distributed metallic cations and with solvated interlamellar anions. The hydrolysis of urea proceeds very slowly but final products provide a better crystallinity and a better control of the particle size. [21] Garcia et

al. also prepared Zn–Ti and Zn–Ce LDHs for the same application.[20] Wei et al. also synthesised Zn–Ti LDHs by the co-precipitation of homogeneous solutions of zinc and titanium salts for dye degradation.[22] They also prepared Ti-based LDH materials by a bottom-up synthesis approach that enhanced the efficiency of the electron–hole separation for visible-light photocatalytic oxygen performance.[23] The same research group also prepared M-Ti-layered double hydroxide matrix (M = Ni, Zn, Mg). [24] ZnAlTi ternary layered double hydroxides with varying Zn:Al:Ti atomic ratios were prepared by the co-precipitation of metal salt solution under low supersaturating conditions.[25] [35] Moreover, our group developed different LDH photocatalysts, such as Zn–Cr LDH, Zn-Fe LDH and Zn-Y LDH, that displayed excellent photocatalytic performance in the degradation of pollutants and decomposition of water under visible-light irradiation. [26] [27] [28] [29] For SnO_2/MgAl LDH, Mg/Al LDH is prepared by the co-precipitation method. [30] Moreover, ternary LDHs prepared by co-precipitation methods with high photocatalytic properties have also been investigated by different research groups. Zn–Al–Fe LDHs with different Zn:Al:Fe ratios showed that Fe^{3+} in the brucite layer of LDHs play a more significant role in the photocatalytic properties. [31-33] In addition, Mg–Zn–Al layered double hydroxides with varying amounts of zinc were prepared by this method.[34] Similarly, Cu/Co–Cr and Zn/Ni–Cr with varying divalent/trivalent metal cation ratios have also been successfully fabricated by co-precipitation method for dye degradation.[35,36] The reconstruction of the original LDH structure by the hydration of the calcined LDH is the unique property, which is attributed to a structural memory effect that can be used to prepare LDH composite photocatalysts. Lu et al. successfully fabricated TiO_2/CuMgAl-R LDHs by this method.[37] The preparation method primarily involved the co-precipitation, calcination and rehydration processes.

2.2. Solution mixing method

The solution mixing method is widely applied to prepare semiconductor/LDH composite photocatalysts. Carja et al. fabricated a novel bi-component photoresponsive nanocomposite (TiO_2/Zn LDH) consisting of zinc-based anionic clay (Zn LDH) and TiO_2 nanoparticles, which was obtained by the structural reconstruction of the Zn LDH in a $TiOSO_4$ aqueous solution.[38]The SnO_2/MgAl composite was prepared by mixing the two semiconductor oxides as ZnO/SnO_2.[30]Valente et al. prepared the CeO_2/ Mg–Al LDH composite by mixing the Mg–Al LDH and cerium nitrate solution under vigorous mechanical stirring.[39] The TiO_2/Zn–Al LDH nanocomposite photocatalyst was prepared by mixing TiO_2 with thermally treated Zn–Al LDH in the Na_2CO_3 solution. [25] Hwang et al. reported the mesoporous layered TiO_2/Zn–Cr LDH composites by mixing the formamide suspensions of Zn–Cr-LDH and layered titanate nanosheets under a constant stirring at room temperature.[40] Recently, they have also reported the synthesis of highly efficient Zn/Cr-LDH graphene nanohybrid composites for visible-light-induced O_2 generation by mixing the formamide suspensions of Zn/Cr-LDH and GO/RGO nanosheets under a constant stirring at room temperature.[41] Carja et al. synthesised the CuO/LDH composite photocatalyst during the structural reconstruction method in the aqueous solution of Cu $(CH_3COO)_2$. They showed that the nanoparticles of CuO are deposited on the surface of the LDH indicating the formation of CuO/clay heterojunctions.[42]The composite Au/Zn–Al LDH and Au/Zn–Ce–Al LDH are synthesised by vigorous stirring of appropriate $AuCl_3$ with the LDH for hydrogen production by solar light irradiation.[43]

2.3. Anion-exchange method

The anion-exchange method is based on the exchange properties of the interlayer anions of LDHs. When the co-precipitation method is unsuitable, the anion-exchange method is used. For example, when the metal cations or the anions are unstable in alkaline solution or the direct

reaction between cations and guest anions is more favourable or if the suitable soluble salt of the guest anions is not available, this method is especially useful. The anion exchange in LDHs primarily depends on the electrostatic interactions between the brucite sheets and the exchanging interlayer anions.[44]

The anion-exchange process in LDHs is associated with the following main features:

(1) Appropriate solvent will favour the anion-exchange process.

(2) The pH value should be more than 4.0; at low pH value, the brucite hydroxyl layer will be vanished.

(3) The anion-exchange process depends on the chemical composition of the LDH host layers.

(4) Generally, higher temperatures favour anion exchange.

The polyoxometalates (POMs) pillared LDHs are generally difficult to synthesise because of the large anionic size. Only ion-exchange method is suitable for synthesising POM intercalate LDHs. We used a facile anion-exchange method to prepare heteropoly acid intercalated Zn/Al LDHs.[45] As polyoxometalate possesses high reduction potential and optoelectronic properties, it plays an important role in the photocatalysis. Hu et al. prepared tungsten polyoxometalates pillared layered double hydroxide by the ion-exchange method for the degradation of organic pollutants. They also synthesised 'paratungstate A' ion intercalated Mg/Al layered double hydroxide by the same method for the photocatalytic degradation of organochlorine pesticides and hexa chloro cyclohexane.[46,47] Fan et al. synthesised a bifunctional Ag/AgBr/Co–Ni–NO_3 LDH nanocomposite photocatalyst by using the facile anion-exchange and light reduction methods. Co–Ni–Br LDH sheets were prepared by a topochemical synthesis method and followed by the addition of the $AgNO_3$ solution to the suspension of Co–Ni–Br LDH. Ag^+ reacted with the LDH interlayer Br^- and was converted to AgBr nanoparticle on the surface of

the LDH sheets; NO_3^- entered the LDH interlayers and followed by light reduction; and Ag/AgBr/Co–Ni–NO_3 LDH nanocomposites were formed.[48]

In addition to the above methods, other methods have been established for the fabrication of different LDHs, such as hydrothermal synthesis, the sol–gel process [49] and the salt–oxide (or salt-hydroxide) method.[50] In addition, for actual practical applications, layered double hydroxide materials are synthesised using nucleation and aging steps, and also microspheres of the material are formed in a subsequent spray drying process.[51- 53] Moreover, other methods are the non-anion-exchange methods that include the microemulsion method,[54] etc., which are used only in special cases.

3. LDH as a Novel Photocatalyst

Over the past two decades, there has been an extremely rapid growth in the publications related to the TiO_2 as a model semiconductor photocatalyst to produce H_2 from water splitting, biomass reforming, industrial waste reforming, and to produce carbon-based solar fuels via CO_2 photoreduction.[55] As TiO_2 absorbs only UV light (up to 380 nm), which is an inherent limitation for the TiO_2-based photocatalysts for efficient light harvesting capacity with low efficiency in the visible region. In the search of other semiconductor materials with photocatalytic activity under visible-light irradiation, important efforts have been carried out in the last decade. Consequently, the LDH-based photocatalysts have been developed as one of the most promising candidates to replace the TiO_2-based photocatalysts. As the photocatalytic properties of materials are determined by their structural and electronic properties, it is essential to discuss the factors that influence the LDH photocatalysis process.

3.1 Influence of structural properties

LDHs are a group of anionic clays which are also known as hydrotalcites.[16] The naturally occurring most common LDHs contain Mg^{2+} and Al^{3+} mineral (Talc) with the chemical formula $Mg_6Al_2{\cdot}(OH)_{16}{\cdot}CO_3{\cdot}4H_2O$. Since hydrotalcite is one of the most representative minerals of this group, LDHs are also called 'hydrotalcite-like compounds' with the general formula $[M(II)_{1-x}M(III)_x\ (OH)_2]^{x+}\ [A_{x/n}\ H_2O]^{x-}$, where M(II) and M(III) are the metal cations, A is an intercalate anion (CO_3^{2-}, SO_4^{2-}, NO_3^-, F^-, or Cl^-), though other natural and artificial structural varieties also exist.[57,58] The structure of hydrotalcite is the same as that of the brucite-like $Mg(OH)_2$ structure, which consists Mg^{2+} ions, octahedrally coordinated by hydroxide ions (Figure 1(a)).[59] These octahedral units consist infinite layers by edge-shared octahedrons with the O–H bond perpendicular to the plane of the layers. The divalent and trivalent metal cations found in LDHs primarily belong to the third and fourth periods of the periodic table.[17, 60] There can be various degrees of M^{II} and M^{III} positional ordering in the hydroxide layers depending on the composition and the nature of the cations. LDHs may also contain M^{1+} and M^{4+} cations but these are limited to specific examples such as Li^+, Zr^{+4}, Sn^{+4} and Ti^{4+}.

In LDHs, the metallic cations are arranged in octahedral environment. The cohesive forces between the brucite layer are induced because of (i) the Columbic force of attraction between the positively charged brucite layers and the negatively charged interlayer depending on the layer charges, and (ii) hydrogen bonding between the OH groups of the metal hydroxide in the brucite layer and the oxygen atoms of the intercalated anions depending on the coordination symmetry. For example, the carbonate ion is intercalated with its molecular plane parallel to that of the layered double hydroxide sheets. This mode of coordination maximises the hydrogen bonding between the layer and the interlayer. Considering this conception, a systematic study has been carried out by Kamath et al.[61]

An important structural characteristic of LDH materials is that the M^{II} and M^{III} or M^{IV} cations are distributed in a uniform manner in the hydroxide layers without cluster materials. The host structure of LDH is based on the brucite-like Mg $(OH)_2$ layers of edge-shared MO_6 octahedron. [19, 62] MO_6 octahedron is one of the important factors that affect the photophysical and photocatalytic properties of LDHs. Moreover, due to the high degree of dispersion, the semiconductor nanoparticles show high photocatalytic efficiency. The high dispersion of transition metal octahedron enable the electron transfer and avoid the recombination of electrons and holes.[63,64] It has also been observed that chromium hydroxide shows a strong absorption in the visible-light regions.[65] This implies that it could serve as a potential photocatalytic material. However, no photocatalytic activity with visible-light irradiation has been found for chromium hydroxide due to low efficiency of electron–hole separation or excited electron transfer. However, CrO_6 was observed to be an efficient photocatalyst compared with $Cr(OH)_3$, which was already proved by Wei and co-workers.[66] In M/Ti (M = Cu, Ni, Zn) LDH, a highly dispersed TiO_6 octahedron within a 2D inorganic matrix has been found to be an effective photocatalyst in the field of photocatalytic water splitting and solar-energy conversion.[67]

One of the most effective methods to synthesise the visible-light-driven photocatalyst is the metal ion doping.[68-71] Doping plays an indispensable role in modifying a material. It has been shown that the two metal ions in LDHs and the M–O bonds make them similar to TiO_2 doping materials. Considering that LDHs have two or three different metal ions and the proportion between these metals can be controlled, they are identified as a ‘doped semiconductor’, where ‘higher valent cation’ acts as a dopant. The variation of transition metal ions in the brucite-like layers enables LDHs to show a broad spectrum of photocatalysis, which has been exemplified in the applications of photocatalysis. It was found that the combination of metals, such as Zn/Cr,

Mg/Cr, Zn/Fe, Mg/Fe, Cu/Cr, Co/Cr, Ni/Fe, etc. leads to the photoresponse of these materials in the visible-light region. In addition, doping is an inadequate procedure to add a huge amount of a metal in a semiconductor material. Addressing this issue, recently Garcia et al. have developed a series of visible-light active Zn/M (M = Cr, Ti, Ce) LDH catalysts for water splitting.[20]They showed that an LDH can be considered as a 'doped semiconductor,' if 'Cr' is used as a dopant. Recently, Parida et al. have studied the doped semiconductor-based different types of LDHs.[26-29] Therefore, LDHs act as doped semiconductors and the cation doping in metal octahedral sites of the brucite layers reflected the properties of a doped semiconductor in photocatalysis. For other metal-doped semiconductors, reproducibility is a key factor that makes it difficult to obtain consistent results. Another advantage is that LDHs can be prepared on a large scale.[26]

LDHs consist of positively charged hydroxide sheets and charge-balancing interlayer anions with interlayer bonding. Thus, they can be exfoliated into positively charged 2D nanosheets. The positively charged LDH nanosheets can also be fabricated by layer-by-layer (LBL) assembly with oppositely charged electrocatalytically active species. Therefore, recently Hwang et al. have prepared mesoporous heterolayered photocatalysts, such as Zn/Cr-LDH nanosheets and layered titanate nanosheets by LBL assembly. The hybrid materials act as an efficient photocatalyst due to the effective electronic coupling between cationic and anionic nanosheets and porous structure.[40] They also prepared self-assembly of Zn/Cr-LDH 2D nanoplates with graphene 2D nanosheets that showed better activity than other photocatalysts.[72]

Moreover, the surface OH^- groups of brucite layer react with valence band holes and yield hydroxyl radicals ($OH^{\bullet}$) that have a very high oxidation potential and are considered as an important intermediate for photo-oxidation reactions.[73] An MgAlTi-LDH sample demonstrated to be a very powerful photocatalyst due to a decrease in the size of the anatase nanoparticles in

combination with highly hydroxylated layered surface of LDHs reported as by Seftel et al.[74] It was previously reported that the OH groups in LDHs may favour the titania activity. The surface hydroxyl groups are converted into $HO^{\bullet}$ radicals, which are the reactive oxygen species (ROS) responsible for the dye degradation.[75-77] In addition to the above facts, other factors such as the calcination of LDHs may also have some effect while forming mixed metal oxides or spinels as the main component for various catalysis reactions. These LDH materials can serve as effective, stable, eco-friendly and regenerated photocatalysts in photocatalysis.[78]

The flexible properties of the layered structure in LDHs play an important role in photocatalysis.[79] Compared with bulk photocatalysts without a layered structure, layered materials provide more favourable environment for the diffusion and separation of photoexcited charge carriers. The high activity of these layered compounds is due to the easy migration and separation of the photogenerated charge carriers by the MO_6 octahedron units.[26,69] Yoshsimura et al.[80] found that different H_2 evolution sites in the layered structure lead to totally different photocatalysis from others. For example, we also explained the superior photoactivity of layered Zn/Fe LDHs, Zn/Y-(NO_3, WO_4, MoO_4) LDHs, compared with ZnO materials.[46,47] Moreover, the importance of the layered structure of LDHs must derive from its capability to absorb water and consequent swelling in various degrees. Thus, water should be able to access the intergallery space as well as the external non-gallery surface. This maximises the surface of the catalyst and helps in the photocatalysis.[35] In addition, the LDH acts as a photoassisted semiconductor because photoexcitation that produces mobility of charges in the lamellar structure inducing the formation of photoactive defects.[81]

The uniform distribution of positive charges on the LDH layers assists in the stability of the interlayer anions by the electrostatic host–guest interactions. As the interlayer bonding

between the LDH sheets is relatively weak, LDHs exhibit excellent ability to exchange with interlayer anions. The interlayer space in LDHs plays an important role in improving the photocatalytic activities. The interlayer water and hydronium ions in the interlayer space of the layered materials play a key role in enhancing photoactivity with efficient charge separation.[82]The interlayer galleries of LDHs are capable of accommodating much more bulky anions. It has been reported that the intercalation of large anions enhances photocatalytic activity as compared with original layered oxides. This is due to the interlayer space that facilitates the reaction between the photogenerated charge carriers and the reactant molecules that suppress the charge recombination.[83-84] Parida et al.[26] found that the carbonate intercalated Zn/Cr-LDH shows high and stable photocatalytic activity for water splitting towards hydrogen evolution due to interlayer carbonate. They also compared the activity of nitrate, tungstate and molybdate-intercalated Zn/Y-LDHs.[29] The highest activity was found in molybdate-intercalated LDHs under visible light irradiation. From molecular orbital energy level diagrams, it was predicted that the HOMO of molybdate is nonbonding with fully filled oxygen 2p orbital and the LUMO of molecular orbital contributes to Mo (4d orbital). Thus, the interlayer molybdate anion gets photoexcited representing HOMO → LUMO OMCT spectra and forms e^- and h^+ pairs. These photogenerated holes can oxidise and reduce the organic molecules to form hydroxyl radicals ($OH^{\bullet}$) and the superoxide radicals ($O_2^{-\bullet}$) that lead to mineralising the organic wastes. However, the intercalated anions result in dramatic activity for efficient charge separation. Hu et al.[45,46] clearly explained the role of interlayer anions in LDHs for photocatalytic activity. They synthesised polyoxometalate (POM)-intercalated LDHs for the degradation reaction of an aqueous organochlorine pesticide, hexachloro cyclohexane (HCH). The photocatalytic reaction occurs in the interlayer space of LDHs and the mode of activation of the compound is the

photonic activation that has the more powerful redox ability by forming electron–hole pairs. Therefore, it indicates that the space between the two layers of brucite sheet play the vital role for the reaction of photocatalysis.

3.2 Influence of electronic properties

The study of electronic properties of LDHs is an indispensable step for the understanding of the chemical behaviour of LDH materials among other semiconductors. The electronic structure calculation of LDHs has been carried out by the computational chemists. Sato et al. reported that the layered structure of LDHs is stabilised by the three-centred bridging OH groups of LDHs.[85] If the transition metal cations are coordinated with the weak field ligands (OH groups and OH_2 groups) in the LDH, they can be calculated only in the high-spin state. Roussel et al.[86] explained the cationic order and structure of Zn/Cr–Cl and Cu/Cr–Cl LDHs by X-ray absorption fine-structure study. Both are characterised by two different regions or layers constituted by octahedrons and the interlamellar spaces. Wei et al. provided a detailed electronic structure of LDHs on the basis of the DFT study. In this model, each bridging oxygen atom in metal–oxygen–metal (M–O–M) is set to be bonded to one hydrogen atom of the OH group, and the terminal oxygen atoms are set to be bonded to two hydrogen atoms of the OH_2 group shown in Figure 1(b) and (c). This model has one OH group at the three-centred bridging position, three OH groups at the two-centred bridging position and nine OH_2 groups at the terminal edges.[87]

The metal octahedra in LDHs are connected with each other by a metal–oxygen–metal oxo bridging linkage. The oxo-bridged binuclear linkages constructed in LDHs act as a visible-light-induced redox centre for photocatalysis and also represent MMCT. This refers to the electronic excitation created from one metal to the other. Several years ago, Frei et al. presented the metal oxo-bridging structure of different doped semiconductors and their photocatalytic

activities.[88,89] For the first time, Kang et al.[90] investigated the titanium-embedded layered double hydroxides like M/Ti LDH (M = Ni, Cu) as an oxo-bridged system for photocatalysis. The wide bandgap of titanium oxide is the biggest problem that is solved by synthesising this type of LDHs. Wei et al. synthesised the high dispersed LDH materials for water splitting. They proposed that the metal–oxygen–metal bond of TiO_6 units in Ni/Ti, Zn/Ti and Mg/Al/Ti–LDH would have a significant influence on the electronic structure of the TiO_6 units resulting efficient photocatalytic behaviour. Recently, we have demonstrated the use of MMCT of different LDHs (Zn/Y, Cu/Co–Cr, Zn/Ni–Cr) as a novel type of visible-light absorbing chromophores.[29,35,36] A systematic investigation of the photocatalytical properties of the Co–O–Fe oxo-bridged LDH system was performed by Kim and co-workers.[91]

The efficiency of the photocatalyst depends on the optical properties and position of the redox potential in a semiconductor. The redox potential of a donor species should be more negative than the valence band position of the semiconductor, and the acceptor molecules must have more positive potential than the conduction band. In this regard, LDHs like the Zn/Cr-LDH Cr-3dt_{2g} band lies just below the H^+/H_2 reduction level and the O_{2p} valence band level is more positive than the oxidation potential of O_2/H_2O. Therefore, the hydrogen evolution in Zn/Cr-LDH is due to the excitation of Cr-3dt_{2g} to Cr-3d$_{eg}$, and the oxygen evolution is due to the excitation of O-2p to Cr3d-t_{2g}.[26,71] Zn/Cr-LDH materials show two strong absorption peaks at 2.2 and 3.0 eV corresponding to the d–d transitions of Cr^{3+} ions. After hybridisation of layered titanates with the Zn/Cr-LDH, an electronic transfer exists between LDH and layered titanate leading to the separation of electrons and holes. From the results of electrochemical CV, it was found that the conduction band of Zn/Cr-LDH shows higher positions than the CB of the layered titanate. Therefore, the photogenerated electrons in the Zn/Cr-LDH can migrate to the CB of the

layered titanate, leading to highly efficient result.[90] In the case of Ni/Cr LDHs, the band edge potential of the Cr 3d-t_{2g} (–0.74 V) and Ni-3d-t_{2g} (–0.23 V) bands lies below the hydrogen reduction level. These photoelectrons are easily excited from Cr 3d-t_{2g} → Cr 3d_{eg} and Ni3d t_{2g} → Ni3d_{eg} due to the d–d transition.[36]

4. Photocatalytic Activity of LDHs

4.1 Photocatalytic detoxification of organic pollutants/environmental remediation

Advanced oxidation processes (AOPs) that involve the production of very reactive oxygen species are efficient methods to remove organic contamination.[92] The main advantage of the use of AOPs is to degrade organic dyes and pollutants that cannot be treated biologically. During the photocatalytic process, the photoexcitation of semiconductor surfaces with ultraviolet–visible radiation generates photoactivated electron–hole pairs. As a result, electrons (e^-) migrate to the conduction band and holes (h^+) are produced in the valance band. The holes mediate the oxidation reaction and produce hydroxyl radicals, whereas the electrons mediate the reduction of the dissolved O_2 to form the superoxide radicals. These superoxide radicals are also protonated to form the hydroperoxyl radical ($HO_2^{\bullet}$) and subsequently H_2O_2. H_2O_2 further decomposes to form the $OH^{\cdot}$ radicals (figure 2). Finally, the radicals formed during this process are responsible for the oxidation of the organic molecules that produce intermediates, H_2O and end products. Therefore, the resulting hydroxyl radicals ($OH^{\bullet}$) with a standard redox potential E^0 = 2.8 V versus NHE, being a strong oxidising agent than other conventional oxidants such as ozone (E^0 = 2.07 V), hydrogen peroxide (E^0 = 1.78 V), chlorine dioxide (E^0 = 1.57 V), chlorine (E^0 = 1.36 V), etc. can react with almost all organic aromatic compounds. Consequently, the photocatalytic processes can be applied to hazardous non-biodegradable water contaminants.[93]

4.1.1. Degradation of organic dyes and pesticides into LDHs

Recent research on the chemistry of LDHs shows their potential applications in the photocatalytic degradation of organic pollutants such as phenolic derivatives, carboxylic acids, xanthene group of dyes, azo-group of dyes or chlorinated aromatics into harmless products, e.g. carbon dioxide, water and simple mineral acids. LDHs exhibit high activity of organic compound degradation under visible light irradiation. Some of the factors that are involved in the LDH photocatalysis process are discussed in part 3 of this review article.

Binary and ternary LDH materials

Mantilla et al. were the first to report the photoassisted degradation of 4-chlorophenol and *p*-cresol by using Mg/Al hydrotalcites. Mg/Al hydrotalcites are not semiconductors, but because of their high photocatalytic activity they are known to perform as an induced semiconductor and termed as a photoassisted system instead of photocatalysis by the authors.[81] In this case, in the laminar structure of layered double hydroids (LDHs), the induced photoexcitation can cause mobility of charges and form the photoactive defects. The number of photoinduced centres could depend on the Mg/Al ratio. The activity of LDHs is enhanced with the increase in the Mg/Al ratio. This work could provide guided information for steering in the design of LDHs with tunable photocatalytic activity. We have fabricated different anions (carbonate, nitrate and chloride) that intercalated Zn/Fe LDHs for the photocatalytic decomposition of azo dyes (methyl violet and malachite green) under solar light irradiation. In this case, the Fe^{3+} ions of edge-shared FeO_6 octahedrons play an important role in visible-light absorption. The LDHs with intercalated carbonate ions have shown highest photocatalytic activity compared with chloride/nitrate-intercalated LDHs because of the narrow and regular pore size distribution, well-defined mesoporosity with narrow band-gap energy and average crystallite size.[29]

During the past decade, lots of work has been developed to modifying TiO_2 by doping with elements such as N, C, and other transition metal ions.[94-96] As compared to pure TiO_2, the modified TiO_2 have been exhibited favourable visible-light absorption and photocatalytic activity. It was found that the C–N–TiO_2 photocatalyst decomposed 10 mg/ L of methylene blue completely in 3 h under UV light irradiation and 50% under visible light irradiation. [97] Subsequently, Shao et al.[22] synthesised Zn/Ti layered double hydroxides considering different Zn/Ti ratios using co-precipitation methods for the decomposition of methylene blue (MB) under visible-light irradiation. The photocatalytic activity depends on the influence of the molar ratio of Zn/Ti. It was found that, under visible-light irradiation, all Zn–Ti LDHs (2:1, 3:1 and 4:1) display high photocatalytic activity than that of commercial TiO_2 and ZnO. Particularly, the photocatalytic activity of the Zn/Ti (3:1) LDH attained ~100% in 100 minutes, which is significantly higher than that of the Zn/Ti (2:1) LDH (~95%) and the Zn/Ti (4:1) LDH (~96%), respectively. It was observed that the Zn/Ti (3:1) LDH display superior activity because of high specific surface area, hierarchical structure and low band-gap energy. In the recent past, Ni et al. synthesised a series of Zn/M–NO_3-LDHs (M = Al, Fe, Ti) and Fe/Ti LDHs for the photocatalytic degradation of Rhodamine B. Amongst these materials, Zn/Ti–NO_3-LDHs showed the best activities because of their hierarchical structure, small crystallite size and high specific surface area.[98] Moreover, Ni/Ti-LDHs are synthesised by using urea as a template and a basic precipitation agent play a vital role for the photocatalytic degradation of methylene blue dye. As compared with ZnO, ZnS, NiO, TiO and Degussa P25, the as-prepared LDH display high activity because of its high specific surface area, porous structure, lower band gap, different surface states of Ni and Ti in the layered framework and in the presence of defects.[99] They also

synthesised Co/Ti (2:1) LDHs by the same procedure for the degradation of aqueous Congo Red.[100]

Several studies have reported the use of the chromium-based transitional metal octahedron of inorganic materials in photocatalysis. In a very recent report, we have explored the application of Zn/Cr LDHs in the photocatalytic degradation of dyes (xanthene dyes) and substituted phenol (4-chloro 2-nitro phenol). As the LDH is based on brucite-like layers with edge-shared $M(OH)_6$ octahedrons, Cr^{3+} ions in the CrO_6 octahedron of Zn–Cr–CO_3 LDHs play an important role in photocatalysis.[26] Wei and co-workers[66] systematically synthesised a group of visible-light-responsive Cu/Ni/Zn–Cr LDHs by using a scale-up method, which exhibited a remarkable activity for Sulpho Rhodamine B, Congo Red, chlorinated phenol and salicylic acid under visible-light irradiation. Due to the high dispersion of the CrO_6 unit in the LDH matrix, M-Cr/NO_3-LDHs (M = Cu, Ni) exhibit 20 times higher photocatalytic activity than the commercial TiO_2 as well as super recyclable ability. However, the band energy analysis demonstrated that M–Cr/NO_3-LDHs show a visible-light response that originates from the d–d transition in the orderly dispersed CrO_6 octahedron in the LDH layer. The effective photocatalytic activity of Cu/Cr LDHs can be attributed to the surface electric property, small energy gap and large number of surface hydroxyl groups as confirmed by the ESR technique. The mechanism was also explained by the HOMO–LUMO concept. Cu/Cr provides two absorption bands: the first one is due to $^4A_{2g}(F) \rightarrow {}^4T_{1g}(F)$ at 410 nm and the second is due to $^4A_{2g}(F) \rightarrow {}^4T_{2g}(F)$ at 570 nm. It was found that the high dispersion of the CrO_6 octahedron in the LDH layers, the low band gap and the surface OH groups of brucite layers play an important role in photocatalysis. A Cu–Cr layered double hydroxide (Cu/Cr-LDH) film by the electrophoretic deposition method was synthesised; and its visible-light-driven photocatalysis for the degradation of organic pollutants

(2, 4, 6-TCP, SRB and Congo red) was studied. Due to the large specific area and the rich macroporous/mesoporous structure, the LDH film shows superior photocatalytic activity compared with the corresponding LDH powder sample.[102] Recently, Parida and co-authors demonstrated a visible-light active carbonate intercalated M^{II} (Co, Ni, Cu and Zn)/$Cr^{III}CO_3$ LDHs for the degradation of methyl orange. The results of the present study demonstrated the effect of M^{II} metal in the brucite layer of $M^{II}/Cr^{III}CO_3$ LDHs in photoactivity.[103] In addition to binary LDHs, a series of carbonate-intercalated Cu−Co/Cr ternary LDH materials was prepared and the effect of divalent metal ions in the brucite layer on the photocatalytic activity was investigated.[35] As the presence of CrO_6 performs a similar role in all the as-prepared Cu/Co–Cr LDHs, we have correlated copper and cobalt concentrations with the photocatalytic activities for different LDHs. The maximum amount of cobalt and the minimum amount of copper in the brucite layer exhibit the highest photocatalytic activity because of the cooperative effect of binary cations and the high electron-transfer ability of cobalt. The reduction potential of Co (E^0, Co^{2+}/Co = −0.28 V) lies at a higher level than that of Cu (E^0, Cu^{2+}/Cu = +0.34 V) and the reduction potential of cobalt is also slightly near to that of oxygen (E^0 = −0.13 V), which can transfer more electrons to the surface-absorbed oxygen to form superoxide radicals. The presence of Cu is also helpful because it helps in forming more and more hydroxyl radicals in the aqueous solution. Frei et al. explained the metal oxo-bridging structure of Ti–O–Cu and Ti–O–Sn using the conception of the metal-to-metal charge transfer spectra (MMCT) for the mechanism of photocatalysis.[88,89] Therefore, to meet the requirements of high performance for photocatalysis and the presence of M^{n+}–O–M^{m+} oxo-bridged bimetallic linkages between two neighbouring LDH octahedra, we introduced a new mechanism. The oxo-bridged binuclear Cr^{III}–O–Cu^{II}/Co^{II} linkages present in LDHs are considered as a visible-light-induced catalytic redox

centre. By the excitation of the oxo-bridged system of Cr^{III}–O–Cu^{II}/Co^{II} under visible-light irradiation, the surface-adsorbed oxygen molecules could be reduced to superoxide radicals, which are reactive oxygen species responsible for the degradation of malachite green.

Calcined LDH materials

It is well known that when the LDH is calcined the layered structure of LDH collapses and a highly dispersed mixed oxide solid solution is formed.[103] As it has been reported that ZnO can be used as a successful photocatalyst for the degradation of organic pollutants.[104] Ahmed et al. synthesised a highly crystalline ZnO from the calcined product of Zn/Al-LDHs for photocatalysis.[105] Similarly, Seftel et al. prepared calcined and uncalcined Zn/Al-LDHs with different cationic ratios by the co-precipitation method for the degradation of methyl orange in the aqueous solution. The result showed that Zn/Al-LDH (Zn:Al = 4) calcined at 500 °C showed 93% MO dye degradation activity in 4 h under UV irradiation. The significant improvement was due to the formation of large amounts of the ZnO phase.[106] On the other hand, Morimoto et al. reported the photodegradation behaviour of methyl orange (MO) and fast green (FG) for calcined Zn/Al and Mg/Al layered double hydroxides. The best result was obtained for the adsorption capacity and photocatalytic activity of Mg_3Al-LDH with the lowest particle size. Consequently, this compound showed dual properties, adsorption and degradation.[107] ZnO-coated flaky layered double hydroxides and flaky mixed-metal oxides (FMMO) were prepared by Zhi et al. for the photocatalytic decomposition of acid red G. The ZnO nanoparticles were homogeneously deposited on the FLDH surface by the co-precipitation method. The results showed that the flaky structure of mixed-metal oxides provides the best result in the adsorption and photodecomposition processes.[108] Mantilla et al. synthesised calcined and uncalcined Zn–Al–Fe LDHs with different Zn:Al:Fe ratios by the co-precipitation method for the degradation of 2,4-

dichlorophenoxyacetic acid (2,4-D). The samples calcined at 673 K showed high adsorptive and high photodegradation activities.[32] They also successfully presented the synthesis of Zn^{2+}/Al^{3+}+Fe^{3+} LDHs with the Al^{3+}/Fe^{3+} ratios of 5.42, 1.36, 1.08 and 0.57, respectively, from the soluble salts and calcined at different temperatures to form mixed oxides designed for the photodegradation of phenol and cresol in the aqueous medium. The obtained mixed oxides showed important properties for semiconductors with high specific surface area and a band gap of 2.54–2.04 eV. For the photodegradation of phenol and *p*-cresol (40 ppm), the high degradation values (98%) were obtained at an Al/Fe ratio of 0.57 after 6 h and 4 h of irradiation, respectively.[81] Zoua et al. used a series of ternary Zn-doped Mg–In-layered composites for the degradation of organic dye [methylene blue (MB)] under visible-light irradiation. By increasing the content of Zn^{2+} in the brucite layer, the crystallinity of the materials decreased because the ionic size of Mg^{2+} and Zn^{2+} does not match with each other. Both as-synthesised and calcined LDH materials showed more activity than In_2O_3 solid and binary Mg–In LDHs. The cause of degradation was the dye-sensitised mechanism and the complex photocatalytic mechanism of semiconductor oxides.[109] For the degradation of C. I. Basic Blue 3 dye, the UV active Mg–Al–Zn mixed-metal oxide photocatalysts derived from Zn $(OH)_2$/Mg–Al LDHs were synthesised. The high crystallinity of the nanocomposite showed better photostability and lower defects which enhanced the photoactivity.[110] Some groups also reported calcined Mg–Zn–Al layered double hydroxides (MgAlZn LDHs) in a co-current down flow bubble column photoreactor at a pilot scale for the photodegradation of 4-chlorophenol (4CP).[111]

As ZnO has a wide band gap and In_2O_3 has a narrow indirect band gap, Li et al.[112] reported a heterostructured Zn–Al–In mixed-metal oxide (ZnAlIn-MMO) nanocomposite photocatalyst from ZnAlIn-LDH precursors for the degradation of methylene blue under visible-

light irradiation and compared it with pure In_2O_3. As compared to pure In_2O_3, it was found that the nanocomposite exhibited much higher photocatalytic activity. It was due to the efficient separation and transformation of the photogenerated electrons and holes that originate the heterostructure of the ZnAlIn-MMO catalyst and in this case the large specific surface area also played an important role. Theyalso synthesised a visible-light-responsive MgO/ZnO/In_2O_3 mixed-metal oxide (MZI-MMO) heterostructured photocatalyst from the LDH precursor for the decomposition of organic dye. [113]

In addition, novel ZnO/$ZnAl_2O_4$ nanocomposites with homogeneously dispersed $ZnAl_2O_4$ nanoparticles inside a network of ZnO are fabricated by the thermal treatment of a single-source precursor of ZnAl-layered double hydroxides (ZnAl-LDHs) as reported by Zhao et al. By adjusting the molar ratio of $Zn^{2+/}Al^{3+}$ to 3:1, the optimised concentration of ZnO and $ZnAl_2O_4$ in the final nanocomposites led to the enhanced photocatalytic activity. For ZnO, the bottom of the CB lies at –4.19 and the top of the VB lies at –7.39 eV, and for $ZnAl_2O_4$, the bottom of the CB and the top of the VB lie at –3.36 and –7.16 eV, respectively, versus the absolute vacuum scale. Therefore, the electrons at the bottom of the CB band of $ZnAl_2O_4$ would migrate to that of the CB of ZnO and holes from top of the VB band of ZnO would migrate to that of $ZnAl_2O_4$. The photogenerated e^- and h^+ pairs can be efficiently separated and they enhance the photocatalytic activities of the ZnO/$ZnAl_2O_4$ nanocomposites.[114]

LDH-based nanocomposites

A composite semiconductor material is formed by combining two or more materials that often exhibit very different properties. In the composite system, when a semiconductor with a large band gap is coupled with more negative CB level of a small band-gap semiconductor, the photogenerated holes are trapped in the small band-gap semiconductor and the CB electrons can

be injected from the small band-gap semiconductor to the large band-gap semiconductor in the presence of light. Thus, an effective charge separation can be obtained. TiO_2 has a wide band gap (3.03 eV for the rutile form and 3.18 eV for the anatase form) with a great ability to produce powerful reactive oxygen species by absorbing photons in the UV region, which greatly limits their practical applications. In comparison to TiO_2, when coupled with the calcined Mg/Al LDH this limitation can be overcome, showing superior photocatalytic performances. Therefore, Valenzuela et al. prepared TiO_2/MgAl LDH nanocomposites by the sol–gel method using ultrasound irradiation during the hydrothermal treatment step for the degradation of phenol. The OH groups in the LDH surface may favour the titania activity. When the amount of hydrotalcite:titania was increased to 1.5:1 and 2:1, the activity decreased as compared to pure TiO_2. This is probably due to the excess of hydrotalcite that covers the TiO_2 nuclei and hinders the formation of the OH radicals. A proposed mechanism for the decomposition of the photocatalytic phenol in the presence of a mixture of TiO_2/Mg–Al layered double hydroxides has been shown in Figure 3.[59]

Carja et al. prepared TiO_2/Zn–Al LDH nanocomposite for the degradation of phenol. The photoresponsive performances of this nanocomposite might originate because of the high surface area and mesoporous properties. Furthermore, the favourable electron-transfer properties of these materials are because of the heterojunction properties of the TiO_2/ZnAlLDH semiconductor. These properties enhance the ability of generating and separating the photoinduced electron–hole pairs.[38] As ceria plays an important role in the photocatalytic process under visible-light irradiation,[115] Jaime S. Valente described the photocatalytic properties of the CeO_2-supported Mg/Al LDH system under UV irradiation for the removal of phenolic compounds using the charge-transfer mechanism .[39]

A new type of nanocomposite SnO_2/Mg–Al-LDH was prepared by wet impregnation of the dehydrated Mg/Al-hydrotalcite-type compounds in an ethanolic solution of $SnCl_4 \cdot 2H_2O$ for the photocatalytic degradation of methylene blue.[30] It followed the photosensitised degradation pathway mechanism. In this case, methylene blue is able to absorb photons and transfer the excited electrons into the SnO_2 conduction band under UV irradiation because of the negative shifting of the flat band potential of SnO_2. Similarly, Seftel et al. also modified the parent Zn/Al-LDHs by incorporating Sn^{IV} in the brucite-like sheet using the co-precipitation method at a constant pH by the total replacement of the trivalent Al^{3+} cations and converted them to Zn/Sn LDHs. In order to obtain a nanosized-coupled ZnO/SnO_2 catalyst, the as-synthesised Zn/Sn-LDH (4×10^{-5} M) was exposed to a thermal treatment for the degradation of methyl orange. The composite with appropriate band levels facilitates the electron–hole transfer between the two semiconductors and the efficiency of the charge separation is increased, showing better photocatalytic activity.[116]

Wei et al.[117] synthesised a biomorphic hierarchical mixed-metal oxide (MMO) framework from LDHs by using a bio-template synthesis method for the decomposition of Sulpho Rhodamine B (RB) and azo-benzene-containing dyes (PAZO). In this work, one kind of legume was chosen as the bio-template. It was found that the bio-template Zn/Al-MMO framework exhibits 2.4 times higher BET specific surface area and much wider pore size distribution with hierarchical structure, which results in enhanced photocatalytic performances than the Zn/Al MMO powder prepared without bio-template.

Li and co-workers reported the Zn/Al-layered double hydroxide/carbon nanotube (Zn/Al-LDH/CNT) nanocomposite through noncovalent bonds in the presence of L-cysteine molecules.[118] Zn/Al-LDH/CNT nanocomposites exhibited excellent performance for the

photodegradation of methyl orange molecules under UV irradiation. Wang et al. described the ZnO nanorods decorated on the calcined Mg–Al layered double hydroxides as photocatalysts with a high adsorptive capacity as well as the photocatalytic properties of the anionic dyes such as acid red.[119] The photocatalysts with magnetic properties have also been introduced in the preparation of magnetically separable LDH-based photocatalysts, which effectively and readily remove the catalysts. Chen et al.[120] successfully fabricated a novel magnetic Fe_3O_4/Zn–Cr-layered double hydroxide composite using a two-step microwave hydrothermal method. The composite decomposed 95% of methylene blue (MB) under UV irradiation. A higher removal of dye by the composite compared with that of Zn/Cr-LDH under the same conditions was due to its high adsorption capability and special nanostructure.

Recently, Hou et al. have synthesised Bi_2MoO_6/Zn/Al LDH hierarchical heterostructures assembled from Bi_2MoO_6 hierarchical hollow spheres and Zn/Al LDH nanosheets by using a low-temperature hydrothermal method. The photocatalytic activity of the Bi_2MoO_6/Zn/Al LDH composites was investigated for the degradation of Rhodamine B. As Zn/Al LDH cannot be excited by visible light, in the case of the heterostructured Bi_2MoO_6/Zn/Al LDH composite, the conduction band (CB) of Zn/Al LDH (+0.55 eV) is more positive than that of Bi_2MoO_6 (−0.31 eV). Therefore, Zn–Al LDHs can accept photogenerated electrons from the CB of Bi_2MoO_6 and can then consequently reduce O_2, decreasing the electron–hole recombination. The composite with LDHs showed better photocatalytic activity and degraded 99% of RhB in 80 minutes, while with Bi_2MoO_6 it was degraded less than 50%.[121]

Employing various heterostructured catalysts, the Cu-doped TiO_2 nanoparticle-supported Cu/Mg/Al-LDHs were successfully synthesised recently by the co-precipitation method and it has been followed by the calcination and the rehydration process of the layered double hydroxide

(CuMgAlTi-LDH) precursor for the photodegradation of MB. In this case, the anatase-type TiO_2 nanoparticles are homogeneously distributed on the surface of the reconstructed CuMgAl-RLDH.[122] The TiO_2/LDH heterojunction nanostructure helps in the separation of the photogenerated electrons and holes, and improves the photocatalytic activity.[38] Cui et al. synthesised silver orthophosphate immobilised flaky Mg/Al (3:1) layered double hydroxides as the visible-light photocatalyst for the photocatalytic decomposition of acid red G. The superior activities can be attributed to the smaller size, good dispersion of immobilised Ag_3PO_4 and strong adsorption of the dye on the surface of FLDH.[123] For the photodegradation of industrial dyes (drimaren red and drimaren navy), Carja et al. fabricated nanostructured photoresponse nickel with nanoparticle-deposited Mg/Al LDHs and Mg/Fe Al LDHs.[124] These were obtained by the structural reconstruction of Mg/Al LDHs and Mg/Fe Al LDHs in the $NiSO_4$ aqueous solution. It was found that the photodegradation of dyes is greatly enhanced by the deposition of nanosized nickel on the surface of the LDH flakes.

The photocatalysis using different nanoparticles (NPs), such as gold (Au) and silver (Ag), on the surface of the semiconductor greatly influences the optical and catalytical properties of the materials because the surface of AgNPs follows the surface plasmon resonance effect under visible-light irradiation. More recently, Shiyun and co-workers[48] synthesised a novel Ag/AgBr/Co–Ni–NO_3 LDH nanocomposite for the degradation of organic pollutants, where the Ag/AgBr nanoparticles were highly dispersed on the Co–Ni–NO_3 LDH sheets. From the photoexcited AgNPs to the conduction band (CB) of AgBr, the electrons were transferred and trapped by molecular oxygen in solution to form O_2^- and also other oxidative species. Similarly, the photoinduced holes in the VB of AgBr can more easily induce the formation of $OH^{\bullet}$ from the OH groups of the LDHs and help in the degradation of organic pollutants.

Recently, 2D hybrid nanocomposites, including graphene and LDH nanosheets, have attracted significant research interest because of their excellent electronic properties and charge-transfer efficiencies. Moreover, a significant breakthrough was achieved in the photocatalytic degradation of organic dyes under visible light. Wu and co-workers[125] fabricated nanohybrids based on the self-assembling of carboxyl graphene and ZnAl LDH layer-by-layer ordered nanohybrid. After the hybridisation, the electronic coupling between ZnAl-LDH and graphene was supposed to contribute to the efficient spatial separation of the photoinduced charge carriers and to reduce the recombination of e^- and h^+ pairs. Therefore, the hybrid materials exhibited significantly higher photocatalytic activity compared with pristine ZnAl-LDHs. Furthermore, for the first time Li et.al synthesised a highly efficient visible-light-driven hybrid nanocomposite consisting of positively charged ZnCr-LDH nanosheets and negatively charged graphene nanosheets for the photoactivity of the degradation of Rhodamine B. Compared with pristine ZnCr-LDH, the ZnCr-LDH/graphene nanocomposites showed superior catalytic activity and increased the lifetime of the photogenerated charge carriers because of the heterostructure which facilitates the efficient transportation and separation of the photogenerated charge carriers.[126]

Intercalated LDH materials

Oxo-bridged MMCT catalysts absorb visible light as well as near-IR light and also show the photocatalytic behaviour. Many research groups have investigated the use of different oxo-bridged semiconductors to achieve higher visible-light catalytic activities. With particular attention, recently, we have developed Zn/Y-LDH-based oxo-bridged systems for the photocatalytic degradation of Rhodamine 6G under visible-light irradiation.[29] The enhancing photoactivity properties of this system are explained on the basis of the oxo-bridged Zn–O–Y system and the HOMO–LUMO concept. The intercalated tungstate and molybdate play a major

role in enhancing the photocatalytic activities because the interlayer anions get photoexcited to their charge-transfer excited state representing O^{2-} ($2p\pi$) → Mo (4d) or W (5d) assigned as HOMO → LUMO OMCT spectra of the photocatalyst, which is photonic activated by forming e^- and h^+ pairs and various reactive oxygen species for photocatalysis. The molybdate-intercalated LDHs showed the best result compared with the tungstate-intercalated LDHs because the unoccupied Mo (4d) orbital (CB) is positioned at a lower energy level than the W (5d) orbital (Figure 4).

Furthermore, decavanadate-intercalated ZnBi–LDHs were fabricated by the ion-exchange method for the degradation of various organic pollutants under solar light irradiation, which showed a high photochemical stability and photocatalytic activity.[127] The presence of distorted VO_6 octahedron of decavanadate is essential for the photocatalysis because of the large dipole moment of the materials, which could be helpful for the electron–hole separation and reduce the charge recombination. Same group[128] also fabricated Cu (II) phthalocyanine intercalated Zn/Al hydrotalcites with molar ratios of 2.0, 3.0 and 4.0 for the degradation of methylene blue under solar light radiation. The intercalated phthalocyanine complexes perform as photosensitiser and assist in the formation of singlet oxygen, which helps in photocatalysis. Moreover, by adding some additives, such as H_2O_2 and $K_2S_2O_8$, the photodecolorisation of MB significantly increases due to the formation of more amount of singlet oxygen by the decomposition of H_2O_2, while NaCl slows down the process.

4.1.2. Organochlorine pesticide degradation into LDHs

Although some persistent organochlorine pesticides have been banned from agricultural and public health usage during the past few decades, the advanced methods for the effective treatment of the removal of these pesticides is a matter of great concern. Therefore, in the past

decade, the use of different photocatalysts for the environmental clean-up of organic pollutants through photo-oxidation received much attention. As-paratungstate A is a kind of isopoly tungstate with photocatalytic activity, the first modified LDH (intercalation of an aqueous paratungstate A cluster ion into the Mg/Al (2:1) LDH) was synthesised by Guo et al.[46] for the photocatalytic degradation of trace aqueous organochlorine pesticide, hexachloro cyclohexane (HCH), under UV irradiation. The mechanism of degradation signified that the interlayer space is the reaction field and produce the photogenerated $OH^{\bullet}$ radicals. As $OH^{\bullet}$ radicals are strong and unselective oxidant species, they help in oxidative degradation and the mineralisation of organic substrate. They also[47] synthesised the tungsten polyoxometalate paratungstate A $[W_7O_{24}]^{6-}$ ion, the monosubstituted or lacunary Keggin $[SiW_{11}O_{39}Mn(H_2O)]^{6-}$, $[SiW_{11}O_{39}Ni(H_2O)]^{6-}$, the monosubstituted Dawson $[P_2W_7O_{61}Mn(H_2O)]^{8-}$, and the Preyssler $[NaP_5W_{30}O_{110}]^{14-}$ pillared Mg/Al, Zn/Cr and Zn/Al LDHs by anion-exchange reaction for aqueous organochlorine pesticide, hexa-chlorocyclohexane (HCH), degradation. The photocatalytic reaction occurs in the interlayer space of the LDH. By photonic excitation, the POM-LDH is converted to POM-LDH* and an electron and hole are formed. The photoholes react with the surface hydroxyl groups and form hydroxide radicals which are strong and unselective oxidant for degradation of dyes. In the meantime, they also prepared polyoxometalate (POM) intercalated layered double hydroxides and calcined the precursors to form Zn/Al/W (Mn) mixed oxides for the degradation of pollutants.[129] Typical research works on LDH photocatalyst towards photocatalytic degradation of pollutants are shown in Table 1.

4.2. LDH towards light-driven water splitting

For photocatalytic water decomposition processes, water molecules are oxidised by the valence band holes to form oxygen gas and are reduced by the conductance band electrons to form

hydrogen gas, corresponding to a 2 electron reaction. The width of the band gap and the energy levels of the conductance band (CB) and valence band (VB) bands are considered the crucial points in the photocatalysis. The energy level at the bottom of the conduction band determines the reducing ability of the photoelectrons, while the energy level at the top of the valence band determines the oxidising ability of the photo generated holes. However, the CB potential of the catalyst should be more negative than the reduction potential of H^+/H_2 (0 V vs NHE, or -0.41 V vs. NHE at pH=7) and the VB edge should be more positive than redox potential of O_2/H_2O (1.23 V vs NHE, pH = 0 or +0.82 V vs pH =7) for an efficient photolysis reaction and the reduction potential for a certain product depends at a predetermined pH.Therefore, theoretically an energy of 1.23 V is equivalent to a photon energy of 1100 nm is required for the above approach (figure 5).[16, 130-131]

4.2.1. Water oxidation (oxygen production)

Silva and co-workers[20] reported three kinds of Zn-containing (Zn/Ti, Zn/Ce and Zn/Cr) LDHs for oxygen generation through photocatalytic water splitting under visible-light irradiation. The most active material was found to be Zn/Cr LDH with an atomic ratio of 4:2 that exhibits two absorption bands in the visible region at λ_{max} of 410 and 570 nm. It was found that the Cr^{3+} dopant is more effective for enhancing the photocatalytic activity of Zn/Cr LDHs by shifting the light absorbance towards the visible range. The apparent quantum yield for O_2 generation measurement at 410 nm was found to be 60.9% for Zn/Cr (2:1), 15.1% for Zn/Ti and 37.8% for Zn/Ce LDHs, respectively. Although these quantum yields are also quite remarkable, they are significantly lower than Zn/Cr LDHs. In addition, Zn/Cr LDHs exhibit enhanced photocatalytic activity compared with the calcined Zn/Cr LDHs. This is because of the layered structures of LDHs. The layered structures of LDHs are capable of absorbing water, which is

able to access the intergallery space as well as the external non-gallery surface and maximises the surface of the material for the oxygen generation through photocatalysis. To increase the lifetime of electrons and holes, Hwang et al.[41] prepared the layer-by-layer ordering of two kinds of 2D nanosheets of Zn/Cr layered double hydroxide and layered titanate for oxygen generation. The obtained heterolayered nanohybrids showed a strong absorption of visible light and a remarkably suppressed photoluminescence signal, indicating an effective electronic coupling between the two-component nanosheets. The exfoliated nanosheets of LDHs and layered titanate possess opposite layer charges with highly porous structures (Figure 6). Consequently, the heterolayered nanohybrids are fairly active for visible-light-induced O_2 generation with a rate of 1.18 μmol h^{-1} g^{-1}, which is higher than the O_2 production rate (0.67 μmol $h^{-1}g^{-1}$) for Zn/Cr LDH material, that is, one of the most effective visible-light photocatalysts for O_2 production.

Kang and co-workers[90] synthesised titanium-embedded layered double hydroxide catalysts with a constant ratio of divalent and tetravalent metal ions such as (Ni/Ti) LDHs and (Cu/Ti) LDHs (M^{II+}: M^{IV+} = 6:1) for photocatalytic water oxidation. In this study, the structures and the bonding nature of LDHs for a mixed oxide structure of LDHs were investigated. The high surface area and the absorption bands in the visible range of (Ni/Ti) LDHs showed a higher reaction rate and produced 49 μmol O_2 in water oxidation by using 1 μmol of $AgNO_3$ as a sacrificial reagent. In addition, (Cu/Ti) LDHs showed a good reaction rate and produced 31 μmol O_2 under the same condition. As $AgNO_3$ was used as a sacrificial reagent, Ag^+ accepts electrons in order to forbid the recombination reaction, and after a long irradiation time, Ag^+ is converted to silver nanoparticles and also enhances the activities. Therefore, the M–O–M structure of LDHs, bonding nature, the large surface area and visible-light absorbance capacity of LDHs result in the high water oxidation photocatalytic activities under visible light. Recently, Kang et

al. have reported the Co–O–Fe oxo-bridged Co/Fe LDHs with different ratios of transition metals for oxygen evolution under visible light. The brucite layer of LDHs contains more iron resulting in good crystallinity, visible range absorption bands and low charge carrier recombination displaying highest efficiency.[91]

The unique properties of graphene oxide (GO) sheets allow extensive modification with surface functionalities for photocatalysis. The graphene sheets attached to other semiconductor surfaces can efficiently transport electrons and improve interfacial charge-transfer processes. Considering this system, Hwang et al.[41] synthesised visible-light active layered double hydroxide 2D nanoplates with graphene nanosheets to form the nanohybrid structure. In the obtained nanohybrids, the positively charged Zn/Cr LDH nanoplates were immobilised on the surface of the negatively charged graphene nanosheets with the formation of a hybrid structure that increases the visible-light absorption and produces a remarkable depression in the photoluminescence signal. The Zn/Cr LDH/graphene hybrid system (1.20 mmol h^{-1} g^{-1}) unusually showed high photocatalytic activity for the visible-light-induced O_2 generation ($\lambda >$ 420 nm), which is far superior to that of Zn/Cr LDH and its physical mixtures with RGO and GO.

In order to overcome the above-mentioned problems, Wei and co-workers synthesised the heterostructured NiTi-LDH/RGO hybrid nanocomposites with a synergic effect from two functional components towards water splitting into oxygen with a rate of 1.968 mmol g^{-1} h^{-1} and a quantum efficiency as high as 61.2% at 500 nm.[132] After that the hierarchical Co/Ti LDH core–shell nanosphere was fabricated by the hydrothermal synthesis of TiO_2 hollow nanospheres followed by an in situ growth of the CoAl-LDH shell. The strong electronic coupling between the TiO_2 core and the CoAl-LDH shell accelerates the electron–hole separation and increase the

solar light exploitation, producing a high photocatalytic activity for the oxygen production rate of 2.24 mmol g^{-1} h^{-1} under visible light irradiation which is about 9 times higher than TiO_2 nanospheres (0.27 mmol mmol g^{-1} h^{-1}).[133] For the first time, a detail explanation was given about the electronic properties (band structure, density of states [DOS] and band edge placement) of different $M^{II}M^{III}$ LDHs (M^{II} = Mg, Co, Ni and Zn; M^{III} = Al and Ga) for the evolution of photocatalytic oxygen from water. From a theoretical prediction, it was proved that only Co/Al-LDH is an efficient oxygen evolution photocatalyst (O_2 generation rate: 973 μmol h^{-1} g^{-1}).[134]

The latest advancement achieved by our group by designing an efficient composite photocatalysts by coupling of Ni/Fe LDH with metal-free polymeric graphitic carbon nitride (g-C_3N_4), which exhibited photocatalytic activities for both H_2 and O_2 evolution under visible light irradiation in the presence of a sacrificial donor and acceptor. Its band structure allows for both water oxidation and reduction reaction. Since CB of g-C_3N_4 (-1.13 V) is more negative than that of the CB of LDH (-0.60V) and VB of LDH (+1.60V) is more positive than the VB edge potential of g-C_3N_4 (+1.57 V), a heterojunction can be built between LDH and g-C_3N_4 (Figure 7). Under visible light irradiation, the photoinduced electrons of g-C_3N_4 transferred into the CB of LDH, while photoinduced holes of LDH migrated to the VB of g-C_3N_4, leading a spatial electron–hole separation on the Ni-Fe LDH/g-C_3N_4 hybrid system.[135]

These original works gave a nice proof-of-concept for fabrication of different composite materials coupled with LDH for H_2 as well as O_2 production.It is highly looked-for to efficiently trap photogenerated holes for efficient photoelectrochemical (PEC) water oxidation to evolve O_2 on layered double hydroxide catalysts. Li groups reported that a binary Zn/Co-LDH) film directly grown on flexible Ni foil via an electrodeposition method at room temperature which exhibited excellent catalytic activity for electrochemical water oxidation. The activity can be

ascribed to the interconnected two-dimensional (2D) LDH nanosheets vertically grown on the Ni foil-conductive substrate, leading to favourable exposure of available active sites for catalytic reaction.[136] Subsequently, same group report the design and synthesis of a novel ID- TiO_2 array photoanode with an ultrathin over layer of phosphated-Ni/Cr Layered double hydroxide by a photoassisted modification and deposition strategy and achieved 100 % oxidative efficiency for PEC water oxidation over a wide range of potential. Similar to the above, it was found that the Co-Al-LDH@$BiVO_4$ photo anode exhibited extremely PEC performance as compared to $BiVO_4$, which is ascribed to the multiple functionalities and a unique two-dimensional nanosheet structure. [137-138]

4.2.2. Water reduction (hydrogen production)

The LDH-based photocatalysis was first studied by Sato et al.[139] They disclosed the photocatalytic properties of CdS and CdS–ZnS incorporated ino the interlayer of layered compounds such as $H_4Nb_6O_{17}$, $H_2Ti_4O_9$, montmorillonite and layered double hydroxides. The CdS–ZnS mixtures incorporated into the interlayer were capable of generating hydrogen gas under visible-light irradiation in the presence of Na_2S, Na_2SO_3 and/or 2-amino ethanol as a sacrificial donor. The incorporation of the CdS–ZnS mixtures in the interlayer of a semiconductor such as $H_4Nb_6O_{17}$ and $H_2Ti_4O_9$ was superior to those of unsupported CdS–ZnS for hydrogen production. Up to now, many papers have been published on different LDHs using photocatalysis. After the discovery of Zn/Cr LDH for oxygen evolution by Garcia et al., our group [26] fabricated a series of Zn/Cr LDH photocatalysts with varying molar ratios of Zn and Cr (2:1, 3:1 and 4:1) for the evolution of hydrogen gas. Amongst all the as-prepared catalysts, Zn/Cr–CO_3 (2:1) LDH extends the absorption edges to the visible region and exhibits good photocatalytic activity (1732 μmol/3h) without the assistance of co-catalysts compared to Rh co-

catalyst loaded TiO_2 (1497 μmol/h^{-1}) towards hydrogen production. However, the photocatalytic H_2 production rate of Fe-doped TiO_2 and Cr-doped TiO_2 exhibited 15.5 μmol/h and 5.3 μmol/h respectively due to the ability of Fe ions to trap both the charge carriers, while Cr can only trap one type of charge carrier and thus avoiding recombination.[140] A significant photoactivity enhancement of the LDH is due to the presence of Cr^{3+} ion in an octahedral site of the LDH which played an important role under visible-light irradiation in the photoexcitation of electrons from Cr-3dt_{2g} to Cr-3d_{eg} orbitals. Furthermore, the carbonate-intercalated Zn/Cr-LDH photocatalysts for hydrogen generation are more promising than those of neat Zn/Cr LDHs. The carbonate ions decrease the recombination reaction and increase the efficiency of hydrogen production (Figure 8).

In addition to Cr-containing LDHs, very recently, Wei and co-workers have introduced a family of photocatalysts of M/Ti-layered double hydroxide matrices (M = Ni, Zn, Mg) for water splitting into hydrogen.[26] They reported that the highly distributing TiO_6 units are well dispersed in LDH host layers by the network of metal oxygen bonding and the oxo-bridging linkage of octahedrons. It has been demonstrated that the electronic structure is modified by the covalent interaction between TiO_6 and NiO_6. The physicochemical characterisations indicated that the highest crystallinity of the LDH at Ni/Ti = 4:1 results in superior dispersion of TiO_6 units. The ordered dispersion of TiO_6 units affects the separation efficiency of the photogenerated electron and hole carriers, and the high degree of surface defects plays a key role in photocatalytic activity. The structural information about the Ti-containing LDHs serves as trapping sites for electrons and thus improves the electron–hole separation efficiency. In addition, these LDH materials can serve as stable, effective and recyclable photocatalysts for water splitting.[24]

In addition to binary LDHs, we also fabricated a ternary series of Mg/Al + Fe-CO_3 layered double hydroxides with a constant ratio of Mg/(Al + Fe) = 2:1 with advanced physicochemical properties and applied them as photocatalysts for the photocatalytic hydrogen generation from water. In the following work, the Al:Fe ratio was varied from 1:4 to lower iron concentration in the LDH precursor. Amongst all the prepared LDHs, Mg/Al + Fe (10:4 + 1) LDHs contain the optimum amount of iron in the brucite layer producing more amount of hydrogen (301 μmol g^{-1} h^{-1}) under visible-light irradiation in the presence of hole scavenger (aqueous methanol solution), which could be attributed to the favourable surface structure and higher crystalline nature of hydrotalcite. Furthermore, LDHs were found to function as doped semiconductors and Fe^{3+} was shown to be a more effective dopant for enhancing the photocatalytic activity by shifting the light absorbance towards the visible range. However, by increasing the amount of the iron content in the salt solution, the visible-light absorption capacity of the material increased, thereby, increasing the surface area as well as the recombination of the photoinduced charge carriers and decreasing the photocatalytic activity. It was found that a higher concentration of iron in the precursor does not exhibit higher activity. In the case of Mg/Al + Fe LDH, the O2p orbital of FeO_6 octahedron, the valencr band electron excited to the conduction band of Fe^{3+} (3d orbital) and H^+ accepts the electrons in the conduction band producing hydrogen gas. [33]

In a subsequent work, we have further investigated carbonate-intercalated ternary (Ni–Zn/Cr) LDH photocatalysts for water splitting under visible-light irradiation.[36] The incorporation of Ni^{2+} into the brucite layer of Zn/Cr LDHs contributes to the enhancement in the photocatalytic activity. For a better understanding, it was assumed that both Ni^{2+} and Cr^{3+} cations have partially filled 3d orbitals, and the band edge potential of the Cr-3d-t_{2g} (–0.74 V) and Ni-3d-t_{2g} (–0.23 V)

is below the H^+/H_2 reduction level; this play a very significant role in water splitting. On exposure to visible light ($\lambda > 400$ nm), the oxo-bridged bimetallic linkage Zn (II)/Ni (II)–O–Cr (III) functions as a visible-light-induced catalytic redox centre, and the induced MMCT transition of Zn(II)/Ni(II)–O–Cr(III) to Zn(I)/Ni(I)–O–Cr(IV) is able to serve as water splitting sites. Hence, the H^+ ions in the conductance band are scavenged by the excited electrons by the reductant-to-band charge transfer (RBCT) and produce hydrogen gas under visible-light irradiation (Figure 9).

In order to further improve charge-transfer efficiencies, LDH nanosheets can be functionalised with other semiconductors. For example, a novel mesoporous CdS pillared ZnCr–LDH was prepared by Lin and co-workers, which exhibited an excellent photocatalytic activity in the H_2 generation at a rate of 374 mmol h^{-1} g^{-1} with a QE of 42.6% under visible irradiation and at a rate of 2164 mmol $h^{-1}g^{-1}$ with a QE of 48.2% under UV–visible irradiation. CdS is a logical candidate to incorporate into ZnCr–LDH, which improves the photocatalytic activity because of the formation of highly porous texture with high surface area and the depression of the photogenerated charge carriers.[141] The loading of nanoparticle (NP) co-catalysts onto a semiconductor has shown to be a new promising photocatalyst for hydrogen production by water splitting. Carja et al. obtained the self-assembly of Au nanoparticle/mesoporous matrices of layered double hydroxides (Au/ZnAl LDH and Au/ZnCeAl LDH) and their derived mixed oxides for hydrogen generation under solar irradiation. It was found that the Au nanoparticle on the surface of the LDH create surface plasmon resonance (SPR). The SPR effect of "Au" and the composition of the anionic clays are the important parameters for H_2 production by using solar light . The presence of cerium in the LDH layers leads to a larger population of positive $Au^{+/3+}$ on the catalyst surface and enhances the photocatalytic performances.[43] In addition, Xu and co-

workers reported the well-dispersed Pt-loaded layered double hydroxides with immobilised photosensitiser (Rose Bengal, Rhodamine B) for photocatalytic hydrogen evolution with remarkably enhanced activity and stability.[142] In this case, the well-dispersed LDH nanocrystals function as support for immobilising RB photosensitiser and Pt nanoparticles.

4.3. LDHs in photocatalytic CO_2 reduction

The photon energy of sunlight can be converted into electric energy and chemical energy using different photocatalysts.[143] The energy level at the bottom of the conduction band determines the reducing ability of the photoelectrons, whereas the energy level at the top of the valence band determines the oxidising ability of the photo generated holes. For photocatalytic CO_2 reduction, the minimum conduction band energy is higher than that for CO_2 reduction potential and the redox potential levels have to be within the band gap of a chosen semiconductor material. For the reduction of CO_2 in to hydrocarbons, electrons in the semiconductor are required to have more negative redox potential, while holes need to lie on more positive potential level for water oxidation reaction [Equation (3)]. Moreover, a total of 2–8 electrons are required to reduce CO_2 into potential hydrocarbon fuels, which is a much more challenging process compared with water splitting. The following equations [Equations (1)–(10)] illustrate the different pathways for the generation of solar fuels and the related potentials at pH=7. [130-131]

$$\text{Photocatalysts} + h\nu \rightarrow e^- + h^+ \quad (1)$$

$$e^- + h^+ \rightarrow \text{Heat (recombination)} \quad (2)$$

Photooxidation Reaction:	*E^0 Redox (V vs. NHE)*	
$H_2O + 2H^+ \rightarrow \frac{1}{2} O_2 + 2H^+$	0.82	(3)
Photoreduction Reaction:	*E^0 Redox (V vs. NHE)*	
$2H^+ + e^- \rightarrow H_2$	–0.41	(4)

$CO_2 + e^- \rightarrow CO_2^{\bullet -}$ –1.90 (5)

$CO_2 + 2H^+ + 2e^- \rightarrow HCOOH$ –0.61 (6)

$CO_2 + 2H^+ + 2e^- \rightarrow CO + H_2O$ –0.53 (7)

$CO_2 + 4H^+ + 4e^- \rightarrow HCHO + H_2O$ –0.48 (8)

$CO_2 + 6H^+ + 6e^- \rightarrow CH_3OH + H_2O$ – 0.38 (9)

$CO_2 + 8H^+ + 8e^- \rightarrow CH_4 + H_2O$ –0.24 (10)

At present, carbon dioxide is considered as the largest contributor to global warming amongst all greenhouse gases. Several methods have been investigated to reduce the CO_2 concentration in the atmosphere.[144, 145] The use of photocatalysts for the conversion of CO_2 into high-energy-content fuels/chemicals (methanol, hydrogen and methane) has the potential to become a viable and sustainable energy source to fossil fuel.[146] Various LDH materials have also been widely studied for the visible-light photocatalytic conversion of CO_2 into methanol using hydrogen. The zinc and/or copper with aluminium LDHs have been reported to be good photocatalysts for the conversion of gaseous CO_2 into methanol using hydrogen under UV–visible light.[147] The catalyst Zn/Al LDH, with the band-gap energy 5.7, was the most active for the CO_2 photoreduction. The band gap (3.5–5.7 eV) was sufficient to proceed with the reaction steps (CO_2^+ $6H^+ + 6e^- \rightarrow CH_3OH + H_2O$; $CO_2 + 2H^+ + 2e^- \rightarrow CO + H_2O$) at the negative reaction potentials. It was found that in Zn /Al LDHs the major product was CO, which was formed at a rate of 620 μmol h^{-1} g^{-1} with 94 mol% selectivity (0.16% conversion), whereas methanol was the major product formed by the incorporation of Cu in LDH photocatalysts, e.g. at a formation rate of 170 μmol h^{-1} g^{-1} over Zn–Cu–Ga photocatalysts. The methanol selectivity in the case of Zn/Al and Zn/Ga LDHs improved from 5.9 to 26 mol% and 39 to 68 mol%,

respectively, by the inclusion of Cu. The photocatalytic rates can be enhanced to 45% by increasing the light intensity by 2.5 times in comparison to the whole wavelength region. It was found from spectroscopic study that the specific interaction of Cu sites with CO_2 is coupled with protons and photogenerated electrons to form methanol. All these reactions depend upon temperature. The rates obtained using the Zn–Cu–Ga catalysts (170 mmol h^{-1} g_{cat}^{-1}) were accelerated to 310 nmol h^{-1} g_{cat}^{-1} by preheating the catalysts at 423 K under vacuum and further to 490 mmol h^{-1} g_{cat}^{-1} using the Zn–Cu–Ga catalysts consisting of interlayer $[Cu(OH)_4]^{2-}$ anions instead of carbonates. They also described the photocatalytic conversion of carbon dioxide into methanol using the optimised Zn–Cu and Zn–Cu–Ga layered double hydroxide catalysts. A significant breakthrough in the photocatalytic conversion of CO_2 into water over Mg/In LDHs by solar radiation has recently been achieved by Teramura et al.[148] LDHs showed superior activity as compared with other metal hydroxides because of their surface based sites and exhibited high water tolerance for the photocatalytic conversion of CO_2 into CO in the aqueous medium. Amongst various LDHs, the metal ions containing Mg, Co, Ni, Cu, Zn, (divalent cations) and Al and Ga (trivalent cations) showed better effect due to higher absorption capacity and potential for CO_2 reduction. According to the previous report, the Zn-containing system showed good results for CO_2 to CO, whereas the Cu-containing LDH is effective for CO_2 to methanol. They further used CuZnGa-LDHs for the photocatalytic conversion of CO_2 into CH_3OH under visible-light irradiation. In addition, the neat LDHs with variable layer elements, loaded with noble metals (Pt, Pd, Au), showed superior activity.[149] Recently, Xu and co-workers have reported the synthesis of self-assembled carbon nitride and layered double hydroxide material. As compared with the pristine-nitrate-intercalated Mg-Al-LDHs, the presence of Pd co-catalyst in the hybrid material showed excellent photocatalytic activity for CO_2 reduction to CH_4, approximately 2.6

times higher than that observed for the Pd-deposited C_3N_4 material. The CO_2 absorption capacity of Mg/Al LDHs showed highest and improved CO_2 reduction ability.[150] Recently, Tanaka et al. have suggested that because of the high electronegativity of fluorine it can be incorporated into the hydroxide sheets as AlF_6 units, which greatly influence the absorption capacity of CO_2 and clearly improve the CO_2 reduction capacity.[151]

5. Conclusions and prospects

Over the past few decades, continuous efforts have been emphasised on the synthesis, modification and application of the photocatalysis for different semiconductors. This review endeavours to sum up the systematic overview on the recent progress, current status and novel achievements of layered double hydroxides for environmental remediation and water splitting of hydrogen and CO_2 reduction into fuel. We briefly examined the promising results of the binary/ternary unmodified LDHs and modified LDH systems. They exhibited excellent catalytic performance because of their versatile chemical composition with good stability and recyclability nature. In the process of photocatalysis, some major challenges include simplifying the synthesis process with high crystallinity, high dispersive and adequate exposure of the active sites, precise control of particle size and morphology and long-term catalytic stability.

In the process of fabrication, LDH-based photocatalysts are generally subjected to a variety of synthetic methods such as co-precipitation, solution mixing, anion exchange, etc. The co-precipitation method is often preferred because it is very easy, simple and involves inexpensive chemicals or apparatus. Consequently, an additional advantage of LDH prepared by co-precipitation and homogeneous precipitation by urea hydrolysis is that it is easy and can also be scaled up for industrial production. Unfortunately, sometimes LDHs prepared by this method suffer from poor crystallinity and the presence of impurity. The urea hydrolysis method (which is

primarily similar to the co-precipitation method) allows better control of particle size and higher crystallinity than other methods. However, this method is only suitable for the preparation of LDHs with high charge density, that is, it cannot be used to prepare LDHs containing Cu^{2+} and Cr^{3+}. Similarly, the disadvantages of the solution mixing method are the relatively high cost of starting compounds and solvents as well as the great difference between the rates of hydrolysis of alkoxides, which make powder synthesis more difficult and expensive. However, this method is favourable for the synthesis of different types of composites. Due to wide flexibility of the compensating interlayer, the anion-exchange synthetic method is used to intercalate different anions into interlayer galleries. It has been demonstrated that the intercalation of different anions in the interlayer of LDHs is capable of improving their catalytic activity. The disadvantages of the anion-exchange method are that the as-synthesised LDHs usually contain carbonate ions, which generally cannot be de-intercalated as they strongly bind to the brucite layer. Therefore, by using this method it is not possible to obtain the LDH-containing metal ions that precipitate at a high pH.

Though a large variety of LDH compounds with even more than two different metal ions and with several intercalated anions have been synthesised by the above methods, the synthesis of the divalent–trivalent LDHs need some specific considerations. First, the ionic radii of the metal ions should not be too different from those of Mg^{2+}. Second, the metal ratio of the cations, i.e. M^{2+}/M^{3+}, should be between 2.0 and 4.0.[152] Third, although the interlayer galleries of LDHs can be exchanged by the ion-exchange method, the selected anions should not interfere the formation of LDH lattice by precipitation of any of the LDH lattice metals (K_{sp} issues).

Studies to date have shown that some LDH photocatalysts with a single component, such as Mg/Al and Zn/Al, exhibit insufficient efficiency and stability in practical applications,

but the LDHs such as $M^{II/III}O_6$ (M = Cr, Ni, Fe, Cu, Co, etc.) are a new class of superior photocatalysts. It demonstrates that an efficient photocatalyst does not require a co-catalyst-loaded material. As an alternative to other oxide catalysts, because of their physical, structural, electronic and optical properties under visible light, LDH materials can serve as a new family of promising photocatalysts. Furthermore, researchers used many functional materials by intercalating the interlayer of LDHs or prepared different composite systems achieving superior results. Although great progress has been made in the study of LDHs in photocatalysis, the following challenges are still remained unsolved:

1. Synthesised LDH photocatalysts should be used in the energy and environmental issues as killing two birds with one stone. Over the past years, a large variety of LDH-based semiconducting materials have been designed and synthesised by some material scientists, but still the best materials are unknown.

Moreover, the photocatalytic mechanism of LDHs is not fully explained, and the theoretical understanding of band energy and the redox potential is in progress, though it is not required while using LDHs. A fundamental in-depth understanding of many factors, including electronic structure, composition, surface area, crystal structure and morphology for LDHs, systematically needs to be explored. Further investigation is needed for the structural property with quantum efficiency as well as for the durability of the materials. As the properties and functionality of LDHs strongly depend on their unique structures and special synthetic methods, the high quality with phase purity must be followed in their preparation.

2. Developing different water treatment technologies based on LDH photocatalysts will be an interesting but difficult job for the researchers because the generation and disposal of these used composite photocatalysts is a big challenge. The LDH/magnetic oxide

composites can solve the above problems because magnetic materials can be easily separated out using an external magnet and can show dual activities such as magnetic and photocatalytic activities.

The benefits of artificial photosynthesis for the conversion of CO_2 into energy are of great interest to reduce the level of atmospheric CO_2. During the past 30 years, many efforts have been put into the design and development of different photoactive catalysts for water splitting or to convert CO_2 into fuels. Unfortunately, up to now there is no photoactive material that has the required high conversion efficiency to make this technology commercially feasible. The crucial factors, such as band edge potential, morphology and particle size, visible-light absorption range and their long-lived charge carriers, have been explained.

3. Exfoliated layered compounds converted into two-dimensional (2D) nanosheets have attracted challenging research nowadays and opening up innovative fields in photocatalysis. Due to their unique structure, high specific surface area, good transparency, excellent electron conductivity and mobility and high chemical stability, the 2D nanosheets are considered as novel materials.[153-154] Recent studies have demonstrated the advantages of different exfoliated layered materials (nanosheets) such as graphitic carbon nitride, graphene oxide and MoS_2 in facilitating the photocatalytic performance.[155-157] Undoubtedly, C_3N_4-based nanocomposites possess a great potential for environmental and energy-related issues.[158] g-C_3N_4 was also used as a catalyst for the photocatalytic reduction of CO_2 under solar irradiation.[159] A recent study has suggested that 2D-layered transition metal dichalcogenides can be used as an efficient and environmental friendly energy material.[160]

The hybridisation of nanosheet LDHs with other electron accepting species formed binary hybrids, providing a powerful method for further enhancing the photocatalytic efficiency. Beyond binary hybrid systems, the multi-hybrid LDH-based nanostructures may provide extraordinary properties. Ogale et al. have reported a triple-junction-based AuNP/$ZnFe_2O_4$/ZnO system for efficient solar photoelectrochemical water splitting.[161] In addition, the new composite N-doped graphene with CdS nanocomposites has been synthesised for the visible-light water splitting process.[162] The photocatalytic performance of g-C_3N_4 show less efficiency because of the fast electron and hole recombination. Dong and co-workers developed a g-C_3N_4/g-C_3N_4 metal-free isotype heterojunction catalyst for improving the charge separation of the visible-light photocatalysts.[163]This pioneering research work was dedicated to synthesise the LDH-based multi-component nanocomposites for superior performance and practical applications. Moreover, the combination of different Sandwich-like homogeneous Nano sheets with LDH Nano sheets can result in a highly efficient material, which seems to be a perfect structure for the electronic transfer. For these multi-component systems, the theoretical calculation and detailed mechanism are still not very clear.

4. Carbon quantum dots (CQDs) can serve as either photoinduced electron acceptors or donors. The optical, electronic and catalytic properties of such particles are drastically different from bulk catalysts. They can function not only as an efficient photocatalyst but also as a multi-functional photocatalyst to promote their wider visible-light absorption range and separation of electrons and holes as well as to stabilise photolysis semiconductors.[164] In particular, it is worth to emphasise that further studies must be planned using LDH-quantum dot composites to further enhance the photocatalytic properties of LDHs.

Most of such research topics are currently under investigation and will be predicted in the near future. Due to the future trends for further development of this research field, we expect that this review can provide an insightful overview to the readers.

References

1. V. Rives, (ed) Layered Double Hydroxides: Present and Future. 2001, Nova Science Publishers, New York.
2. D. G. Evans and R. C. T. Slade, *Struct. Bond*., 2006, **119**, 1-87.
3. F. Helv. Feitknecht, *Chim. Acta*., 1942, **25**, 131-137.
4. F. Helv. Feitknecht, *Chim. Acta*., 1942, **25**, 555-569.
5. R. Allamnn, *Acta. Cryst. B*, 1968, **24**, 972-977.
6. H. F. W. Taylor, *Miner. Mag*., 1969, **37**, 338-342.
7. F. Cavani, F. Trifirb and A. Vaccari, *Catalysis Today*, I99I, **11**, 173-301.
8. J. Das, B. S. Patra, N. Baliarsingh and K. M. Parida, *Appl. Clay Sci*., 2006, **32**, 252–260.
9. K. M. Parida, M. Sahoo and S. Singha, *J. Catal*., 2010, **276**, 161–169.
10. D. P. Das, J. Das, and K. Parida, *J. Colloid Interface Sci*., 2003, **261**, 213–220.
11. S. Singha, M. Sahoo and K. M. Parida, *Dalton Trans*., 2011, **40**, 7130-7132.
12. N. Baliarsingh, K. M. Parida and G. C. Pradhan, *RSC Advance*, 2013, **3**, 23865-23878.
13. P. Nalawade, B. Aware V. J. Kadam and R. S. Hirlekar, *J. Sci. Ind. Res*., 2009, **68**, 267-272.
14. B. Z. Karan and A. N. Ay, *Chem. Pap.*, 2012, **61**, 1-10.
15. G. Fan, F. Li, D. G. Evans and X. Duan, *Chem. Soc. Rev.*, 2014, **43**, 7040-7066.
16. X. Xiang, F. Li, and Z. Huang, *Rev. Adv. Sci. Eng*., 2014,3,158-171.

17. J. He, M. Wei, B. Y. Li, D. Kang, G. Evans and X. Duan, *Structure and Bonding*, 2006,**119**, 89-119.

18. D. G. Evans and R. C. T. Slade, *Structure and Bonding*, 2006,**119**, 1-87.

19. A. I. Khan and D. O'Hare, *J. Mater. Chem*., 2002, **12**, 3191-3198.

20. G. Silva, Bouizi, Y. Fornes and H. V. Garcia, *J. Am. Chem. Soc.,* 2009, **131**, 13833-13839.

21. U. Costantino, F. Marmottini, M. Nocchetti and R. Vivani, *Eur. J. Inorg. Chem.,* 1998, **10**, 1439-1446.

22. M. Shao, J. Han, M. Wei, G. D. Evans and X. Duan, *Chem. Eng. J*., 2011, **168**, 519-524.

23. Y. Zhao, B. Li, Q. Wang, W. Gao, C. J. Wang, Min Wei, David G. Evans, X .Duana and D. O'Hare, *Chem. Sci*., 2014, **5**, 951–958.

24. Y. Zhao, P. Chen, B. Zhang, D. S. Su, S. Zhang, L. Tian, J. Lu, Z. Li, X. Cao, B. Wang, M. Wei, D. G. Evans and X. Duan, *Chem. Eur. J*., 2012, **18**, 11949-11958.

25. M. H. Kostic, T. Vulic, J. Ranogajec, R. M. Neducin and A. Radosavljevic- Mihajlovic, *J. Therm. Anal. Calorim*., 2013, **111**, 1155-1162.

26. K. Parida and L. Mohapatra, *Dalton Trans*., 2012, **41**, 1173-1178.

27. L. Mohapatra and K. M. Parida, *Sep. Purif. Technol*., 2012, **91**, 73-80.

28. K. Parida and L. Mohapatra, *Chem. Eng. J*., 2012, **179**, 131-139.

29. L. Mohapatra, K. Parida and M. Satpathy, *J. Phys. Chem. C*, 2012, **116**, 13063-13070.

30. E. Dvininov, M. Ignat, P. Barvinschi, M. A. Smithers and E. Popovici, *J. Hazard. Mater.,* 2010, **177,** 150-158.

31. M. F. Tzompantzi, J. L. Fernandez, J. A. I. Diaz Gongora, G. Mendoza and R.Gomez, *Catal. Today*, 2009, **148**, 119-123.

32. A. Mantilla, F. Tzompantzi, J. L. Ferna´ndez, J. A. I. Dıaz Gongora and R. Gomez, *Catal. Today*, 2010, **150**, 353–357.

33. K. M. Parida, M. Satpathy and L. Mohapatra, *J. Mater. Chem*., 2012, **22**, 7350-7357.

34. J. S. Valente, F. Tzompantzi, J. Prince, J .G. H. Cortez and R. Gomez, *Appl. Catal. B Environ*., 2009, 90, 330–338.

35. K. M. Parida, L. Mohapatra and N. Baliarsingh, *J. Phys.Chem.C*, 2012, 116, 22417-22424.

36. N. Baliarsingh, L. Mohapatra and K. Parida, *J. Mater. Chem. A*, 2013, **1**, 4236-4243.

37. R. J. Lu, X. Xu, J. P. Chang, Y. Zhu, S. L. Xu and F. Z. Zhang, *Appl. Catal. B: Environ*., 2012, 111, 389-396.

38. G. Carja, A. Nakajima, S. Dranca, C. Dranca and K. Okada, *J. Phys. Chem. C*, 2010, **114**, 14722-14728.

39. J. Valente F. Tzompantzi and J. Prince, *Appl. Catal. B: Env.*, 2011, **102**, 276-285.

40. J. L. Gunjakar, T. W. Kim, H. N. Kim, I. Y. Kim and S. Hwang, *J. Am. Chem. Soc*., 2011, **133**, 14998-15007.

41. J. L. Gunjakar, I.Y. Kim, J. M. Lee, N. S. Lee and S. Hwang, *Energ. Env. Sci.*, 2013, **6**, 1008-1017.

42. G. Carja, L. Dartu, K. Okada and E. Fortunato, *Chem. Eng. J*., 2013, **222**, 60-66.

43. G. Carja, M. Birsanu, K. Okada and H. Garcia, *J. Mater. Chem. A*, 2013, **1**, 9092-9098.

44. N. Morel-Desrosiers, J. Pisson, Y. Israeli, C. Taviot-Gueho, J. P. Besse, J. P. Morel, *J. Mater. Chem*., 2003, **13**, 2582-2585.

45. J. Das and K. M. Parida, *J. Mol. Catal. A: Chem*, 2007, **264**, 248-254.

46. Y. Guo, D. Li, C. Hu, Y. Wang, E. Wang, Y. Zhou and S. Feng, *Appl. Catal. B*, 2001, **30**, 337-350.

47. Y. Guo, D. Li, C. Hu, Y. Wang and E. Wang, *Int. J. Inorg. Mater*., 2001, **3**, 347-355.

48. H. Fan, J. Zhu, J. Sun and S. Zhang, *Chem. Eur. J*., 2013,**19**, 2523-2530.

49. F. Zhanga, N. Dub, S. Songb, J. Liuc and W. Hou, *J. Solid State Chem.*, 2013, **206**, 45–50.

50. J. Prince, A. Montoya, G. Ferrat and J. S. Valente, *Chem. Mater*., 2009, **21**, 5826–5835.

51. A. de Roy, C. Forano, K. El Malki, J. P. Besse, In Synthesis of Micrporous Materials; Ocelli, M. L.; Robson, M. E., (ed.); Van Nostrand Reinhold: New York,1992, II, 108-169.

52. Y. Wang, F. Zhang, S. Xu, X. Wang, D. G. Evans and X. Duan, *Ind. Eng. Chem. Res*., 2008, **47**, 5746–5750.

53. Y. Zhao, F. Li, R. Zhang, D.G. Evans and X. Duan, *Chem. Mater*., 2002, **14**, 4286-4291.

54. F. Leroux, M. Adachi-Pagano, M. Intissar, S. Chauviere, C. Forano and J. P. Bessea, *J. Mater. Chem*., 2001, **11**, 105-112.

55. Yi Ma, X. Wang, Y. Jia, X. Chen, H. Han, and C. Li, *Chem. Rev*., 2014, **114**, 9987−10043.

56. P. S. Braterman, Z. P. Xu and F. Yarberry, *Handbook of Layered Materials, eds. S.M. Auerbach, K. A. Carrado, P. K. Dutta, Marcel Dekker*, 2004, 373-474.

57. F. Cavani, F. Trifiro and A. Vaccari, *Catal. Today*, 1991, **11**, 173-302.

58. S. Velu, K. Suzuki and T. Osaki, *Catal. Lett*., 2000, **69**, 43-50.

59. S. P. Paredes, M. A. Valenzuela, G. S. Fetter, O. Flores, *J. Phys. Chem. Solids*, 2011, **72**, 914-919.

60. C. Forano, T. Hibino, F. Leroux, C. T. Gueho, Hand book of Clay Science, 2013, **5**, 451-490.

61. S. Marappa, S. Radha and P. V. Kamath, *Eur. J. Inorg. Chem*., 2013, **12**, 2122-2128.

62. G. Hu and D. O'Hare, *J. Am. Chem. Soc*., 2005, **127**, 17808-17813.

63. X. D. Wang C. J. Summers and Z. L. Wang, *Adv. Mater*., 2004, **16**, 1215-1218.

64. J. W. Tang, Z.G. Zou and J. H. Ye, *Angew. Chem*., 2004, **116**, 4563- 4466.

65. K. Maeda, N. Sakamoto, T. Ikeda, H. Ohtsuka, A. Xiong, D. Lu, M. Kanehara, T. Teranishi and K. Domen, *Chem. Eur. J*., 2010, **16**, 7750-7759.

66. Y. Zhao, S. Zhang, B. Li, H. Yan, S. He, L. Tian, W. Shi, J. Ma, M. Wei, D. G. Evans and X. Duan, *Chem. Eur. J*., 2011, **17**, 13175-1318.

67. Y. Zhao, B. Li, Q. Wang, W. Gao, C. J. Wang, M. Wei, D. G. Evans, X. Duana and D. O'Hare, *Chem. Sci*., 2014, **5**, 951-958.

68. X. Chen and S. S. Mao, *Chem. Rev*., 2007, **107**, 2891-2959.

69. E. A. R. Garcia, Y. Sun and D. Raftery, *J. Phys. Chem. C*, 2007, **111**, 17146–17154.

70. L. G. Devi and R. Kavitha, *Appl. Catal. B: Environ*., 2013, **140,** 559-587.

71. G. Liu, L. Wang, H. G. Yang, H. M. Cheng, G. Qing (Max) Lu *J. Mater. Chem*., 2010, *20*, 831-843.

72. B. Li, Y. F. Zhao, S. Zhang, W. Gao and M. Wei, *ACS Appl.Mater. Interfaces*., 2013, **5**, 10233-10239.

73. M. R. Hoffmann, S. T. Martin, W. Choi and D. W. Bahnemann, *Chem. Rev*., 1995, **95**, 69-96.

74. E. M. Seftel, M. Mertens and P. Cool, *Appl. Catal., B: Environ*., 2013, **134**, 274–285.

75. K. Lv, J. Yu, K. Deng, X. Li and M. Li, *J. Phys. Chem. Solids,* 2010, **71**, 519-522.

76. G. Liu, L. Z. Wang, C. H. Sun, X. X. Yan, X. W. Wang, Z. G. Chen, S. C. Smith, H. M. Cheng and G. Q. Lu, *Chem. Mater*.,2009, **21**, 1266-1274.

77. G. Liu, L. Wang, H. G. Yang, H. M. Cheng, G. Q. (Max)Lu, *J. Mater. Chem*., 2010, **20**, 831-843.

78. M. Zhao, Q. Zhang, J. Huang and F. Wei, *Adv. Funct. Mater.*, 2012, **22**,675-694.

79. X. Lin, T. Huang, F. Huang, W. Wang and S. Jianlin, *J. Phys. Chem. B*, 2006, **110**, 24629–24634.

80. Y. Yoshimura, Y. Ebina, J. Kondo, *J. Phys. Chem.*, 1993, **97**, 1970-1973.

81. A. Mantilla, J. G. Acatitla, G. M. Mendoza, F. Tzompantzi and R. Gomez, *Ind. Eng. Chem. Res*., 2011, **50**, 2762-2767.

82. X. Chen, S. Shen, L. Guo and S. S. Mao, *Chem. Rev*., 2010, **10**, 6503-6570.

83. J. Fang, Z. X. Zheng and Z. Shourong, *J. Hazard. Mater.* 2009,**164**, 250-1256.

84. X. Zong and L. Wang, *J. Photochem. Photobiol. C: Photochem. Rev*., 2014, **18**, 32–49.

85. H. Sato, A. Morita, K. Ono, H. Nakano, N. Wakabayashi and A. Yamagishi, *Langmuir,* 2003, **19**, 7120-7126.

86. H. Roussel, V. Briois, E. Elkaim, A. de; Roy and J. P. Besse, *J. Phys. Chem. B*, 2000, **104**, 5915-5923.

87. Y. Hong, M. Ma, J. Wei, F. Li, D. G. Evans and X. Duan, *J. Phys. Chem. A*, 2009, **113**, 6133–6141.

88. W. Lin and H. Frei, *J. Phys. Chem. B,* 2005, **109**, 4929-4935.

89. W. Lin and H. Frei, *J. Am. Chem. Soc*., 2005, **127**, 1610-1611.

90. Y. Lee, J. H. Choi, H. J. Jeon, K. M. Choi, J. W. Lee, J. K. Kang, *Energy Environ. Sci*., 2011, **4,** 914-420.

91. S. J. Kim, Y. Lee, D. K. Lee, J. W. Lee and J. K. Kanga, *J. Mater. Chem. A,* 2014, **2**, 4136-4139.

92. S. Xu and D. Feng, *J. Phys. Chem. C,* 2009, **113**, 2463-2467.

93. P. R. Gogate and A. B. Pandit, *Adv. Environ. Res. B*, 2004, **8**, 501-551.

94. R. Asahi, T. Morikawa, H. Irie, and T. Ohwaki, *Chem. Rev*., 2014, **114**, 9824–9852.

95. M. Kapilashrami, Y. Zhang, Y. -S. Liu, A. Hagfeldt, J. Guo, *Chem. Rev*., 2014, **114**, 9662–9707.

96. S. A, Ansari, M. M. Khan, M. O. Ansaric and M. H. Cho, *New J. Chem*., 2016, **40**, 3000-3009.

97. X. Yang, C. Cao, L. Erickson, K. Hohn, R. Maghirang and K. Klabunde, *J. Catal*., 2008, **260**, 128-133.

98. S.-J. Xia, F.-X. Liu, Z.M. Ni, J.-L. Xue, P.-P. Qian, *J. Colloid Interface Sci*., 2013, **405**, 195-200.

99. P. R. Chowdhury, K. G. Bhattacharyya, *Dalton Trans*., 2015, **44**, 6809–6824.

100. P. R. Chowdhury and K. G. Bhattacharyya, *RSC Adv*., 2015, **5**, 92189- 92206.

101. L. Tian, Y. Zhao, S. He, M. Wei and X. Duan, *Chem. Eng. J*., 2012, **184**, 261-167.

102. N. Baliarsingh, K. M. Parida and G. C. Pradhan, *Ind. Eng. Chem. Res*., 2014, 53, 3834−3841.

103. J. Rocha, M. del Arco,b V. Rivesb and M. A. Ulibarri, *J. Mater. Chem*., 1999, **9**, 2499-2503.

104. K. M. Parida and S. Parija, *Sol. Energy*, 2006, **80**, 1048-1054.

105. A. A. Ahmed, Z. A. Talib, Zakaria, M.Z. Hussein and A. Zakaria, *J. Alloys Compd*., 2012, **539,** 154-158.

106. E. M. Seftel, E. Popovici, M. Mertens, K. Witte, G. Tendeloo, P. Cool and E. F. Vansant, *Micropor. Mesopor. Mater*., 2008,**113**, 296–304.

107. K. Morimoto, K. Tamura, N. Iyi, J. Ye and H. Yamada, *J. Phys. Chem. Solids,* 2011, **72**, 1037-1041.

108. Y. Zhi, Y. Li, Q. Zhang and H. Wang, *Langmuir,* 2010, **19,** 15546-15553.

109. L. Huanga, S. Chua, J. Wanga, F. Konga, L. Luoa, Y. Wanga and Z. Zoua, *Catal. Today*, 2013, **212**, 81-88.

110. Z. M. Rezvani, A. Sarkarat, R. Khataee and K. Nejati, *Cryst. Res. Technol*., 2012, **47**, 1172-1184.

111. E. M. Campo, J. S. Valente, T R. Pavon, A. Romero, R. Mantilla and R. Natividad, *Ind. Eng. Chem. Res*.,2011, **50**, 11544-11552.

112. G. Fan, W. Sun, H. Wang and F. Li, *Chem. Eng. J.,* 2011, **174**, 467-474.

113. X. Xiang, L. Xie, Z. Li and F. Li, *Chem. Eng. J*., 2013, **221**, 222-229.

114. X. Zhao, L. Wang, X. Xu, X. Lei, S. Xu and F. Zhang, *AIChE Journal*, 2011, **58**, 573-582.

115. N. Wetchakun, S. Chaiwichain, B. Inceesungvorn, K. Pingmuang, S. Phanichphant, I. M. Andrew and J. Chen, *ACS Appl. Mater. Interfaces*, 2012, **4**, 3718–3723.

116. E. M. Seftel, E. Popovici, M. Mertens, E.A. Stefaniak, R. Van Grieken, P. Cool and E. F. Vansant, *Appl. Catal. B Environ*., 2008, 84, 699–705.

117. Y. Zhao, M. Wei, J. Lu, Z. L. Wang and X. Duan, *ACS Nano*, 2009, **3**, 4009-4016.

118. X. Cui, Y. Li, Q. Zhang and H. Wang, *AIChE Journal*, 2009, **56**,768–778.

119. S. Yuana, Y. Li, Q. Zhangb, H. Wang, *Colloids and Surf. A: Physicochem. Eng. Aspect*, 2009, **348**, 76-83.

120. D. Chen, Y. Li, J. Zhang, W. Li, J. Zhou, L. Shao, G. Qian, *J. Hazard Mater*., 2012, **243**,152–160.

121. H. Li, Q. Deng, J. Liu, W. Hou, N. Du, R. Zhang and X. Tao, *Catal. Sci. Technol*., 2014, **4**, 1028-1037.

122. R. J. Lu, X. Xu, J. P. Chang, Y. Zhu, S. L. Xu and F. Z. Zhang, *Appl. Catal. B: Environ*., 2012, **111**, 389-396.

123. X. Cui, Y. Li, Q. Zhang, H.Wang, *Int. J. Photoenergy*, 2012, **2012**, 1-6.

124. G. Carja, E. Husanu, C. Gherasi and H. Iovu, *Applied Catalysis B: Environmental*, 2011, **107**, 253- 259.

125. Z. Huang, P. Wu, B. Gong, Y. Fange and N. Zhua, *J. Mater. Chem. A,* 2014, **2**, 5534-5540.

126. M. Lan, G. Fan, L. Yang and F. Li, *Ind. Eng. Chem. Res*., 2014, **53**,12943-12952.

127. L. Mohapatra and K. M. Parida, *Phys. Chem. Chem. Phys*., 2014, **16**, 16985-16996.

128. K. M. Parida, N. Baliarsingh, B. S. Patra and J. Das, *J. Mol. Catal. A: Chem*., 2007, **267**, 202-208.

129. Y. Guo, D. Li, C. Hu, E. Wang, Y. Zou, H. Ding and S. Feng, *Microporous Mesoporous Mater*., 2002, **56**, 153-162.

130. S. N. Habisreutinger, L. Schmidt-Mende, and J. K. Stolarczyk, *Angew. Chem. Int. Ed*. 2013, **52**, 7372–7408.

131. P. D. Tran, L. H. Wong, J. Barber and J. S. C. Loo, *Energy Environ. Sci*., 2012, **5**, 5902-5918.

132. B. Li, Y. F. Zhao, S. Zhang, W. Gao and M. Wei, *ACS Appl.Mater. Interfaces*., 2013, **5**, 10233-10239.

133. Y. Dou, S. Zhang, T. Pan, S. Xu, A. Zhou, M. Pu, H. Yan, J. Han, M. Wei and D. G. Evans, X. Duan, *Adv. Funct. Mat*., 2015, **25**, 2243–2249.

134. S. M. Xu, T. Pan, Y. -B. Dou, H. Yan, S. -T Zhang, F. –Y. Ning, W. -Y Shi and M. Wei, *J. Phys. Chem. C*, 2015, **119**, 18823-18834.

135. S. Nayak, L. Mohapatra and K.Parida, *J. Mater. Chem. A*,2015, **3**,18622- 18635.

136. Y. Li, L. Zhang, X. Xiang, D. Yan and F. Li, *J. Mater. Chem. A*, 2014, **2**, 13250.

137. W. He, Y. Yang, L. Wang, J. Yang, X. Xiang, D. Yan and Feng Li, *ChemSusChem*., 2015, **8**,1568 –1576.

138. W. He, R. Wang, L. Zhang, J. Zhu, X. Xiang and F. Li, *J. Mater. Chem. A*, 2015, **3**, 17977–17982.

139. T. Sato, K. Masaki and T. Yoshioka, A. *J. Chem. Tech. Biotechnol*., 1993, **58**, 315-410.

140. R. Dholam, N. Patel, M. Adami and A. Miotello, *Int. J. Hydrogen Energ.,* 2009, **34**, 5337–5346.

141. G. Zhang, B. Lin, W.Yang, S. Jiang, Q. Yao, Y. Chen and B. Gao, *RSC Adv*., 2015, **5**, 5823–5829.

142. J. Hong, Y. Wang, J. Pan, Z. Zhongc and R. Xu*, Nanoscale*, 2011, **3**, 4655-4661.

143. Y. Izumi, *Coord. Chem. Rev.*, 2013, **257**, 171–186.

144. J. Hong, W. Zhang, J. Ren and R. Xu, *Anal. Methods*, 2013, **5**, 1086-1097.

145. M. F. Kubacka and G. G. Colón, *Chem. Rev*., 2012, **112**, 1555-1614.

146. N. Ahmeda, M. Morikawab and Y. Izumi, *Catal. Today*, 2012, **185**, 263-269.

147. N. Ahmed, Y. Shibata, T. Taniguchi and Y. Izumi, *J. Catal*., 2011, **279**, 123-125.

148. K. Teramura, S. Iguchi, Y. Mizuno, T. Shishido and T. Tanaka, *Angew. Chem. Int. Ed*., 2012, **51**, 11624 -11628.

149. K. Katsumata, K. Sakai, K. Ikeda, G. Carja, N. Matsushita and K. Okada, *Materials Letters,* 2013,**107**, 138–140.

150. J. Hong, W. Zhang, Y. Wang, T. Zhou, and R. Xu, *ChemCatChem*., 2014, **6**, 2315–2321.

151. S. Lguchi, K. Teramura, S. Hosokawa and T. Tanaka, *Applied Catalysis A: General*, 2015, doi:10.1016/j.apcata.2015.11.023

152. F. Cavani, F. Trifirb and A. Vaccari, *Catalysis Today*, I99I, **11**, 173-301.

153. S. Bag, K. Roy, C. S. Gopinath and C. R, Raj, *ACS Appl. Mater. Interfaces*, 2014, **6**, 2692-2699.

154. K. Bhowmik, S. Pramanik, S. K. Medda, G. De, *J. Mater. Chem.*, 2012, **22**, 24690–24697.

155. X. F. Song, J. Hub and H. Zeng, *J. Mater. Chem.C,*2013, **1**, 2952-2969.

156. J. Xu, L. Luo, G. Xiao, Z. Zhang, H. Lin, X. Wang and J. Long, *ACS Catal*., 2014, **4**, 3302-3306.

157. J. Xu, L. Zhang, R. Shi and Y. Zhu, *J. Mater. Chem. A*, 2013, **1**, 14766-14772.

158. K. Li, S. Gao, Q. Wang, H. Xu, Z. Wang, B. Huang, Y. Dai and Jun. Lu, *ACS Appl. Mater. Interfaces*, 2015, **7**, 9023–9030.

159. D. Guohui and L. Zhang, *J. Mater. Chem*., 2012, **22**, 1160-1166.

160. H. Li, Y. Shi, M.-H.Chiu and L.-J. Li, *Nano Energy*, 2015, **18**, 293–305.

161. A. Sheikh, A. Yengantiwar, M. Deo, S. Kelkar and S. Ogale, *Small*, 2013, **9**, 2091-2096.

162. L. Jia, D.-H. Wang, Y.-X. Huang, A.-W. Xu and H.-Q. Yu, *J. Phys.Chem. C*, 2011, **115***,* 11466–11473.

163. F. Dong, Z. Zhao, T. Xiong, Z. Ni, W. Zhang, Y. Sun and W. -K. Ho, *ACS Appl. Mater. Interfaces,* 2013, **21**, 1392–11401.

164. R. Liu, H. Huang, H. Li, Y. Liu, J. Zhong, Y. Li, S. Zhang and Z. Kang, *ACS Catal*., 2014, **4***,* 328-336.

Figures & Tables

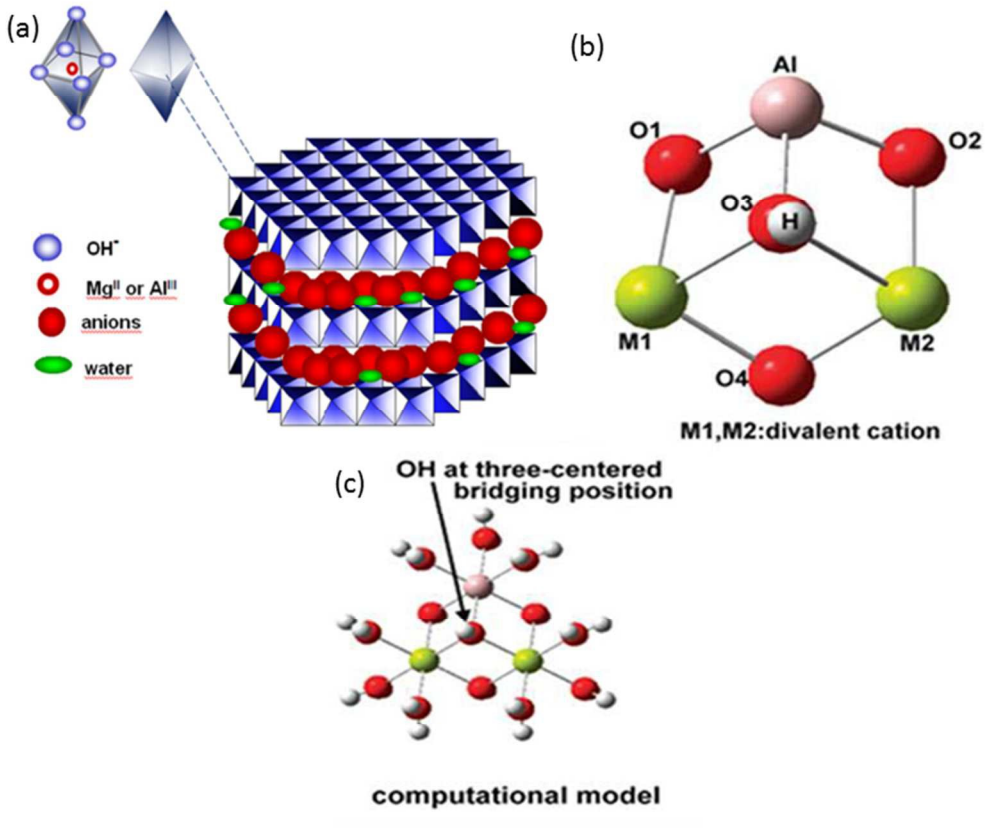

Fig.1(a) Structural ilustration of LDH (b) Computational model of $M_2Al\ (OH_2)_9(OH)_4]^{3+}$ (M_2: divalent metal cation) clusters. (c) One part of the cluster model including the linkage around the three-centered bridging OH group which is used to analyze the calculation data.

("a" adapted with permission from ref. 59 @ copyright 2011 Elsevier Ltd, (b) and (c) adapted with permission from ref. 87 @ Copyright 2009American Chemical Society).

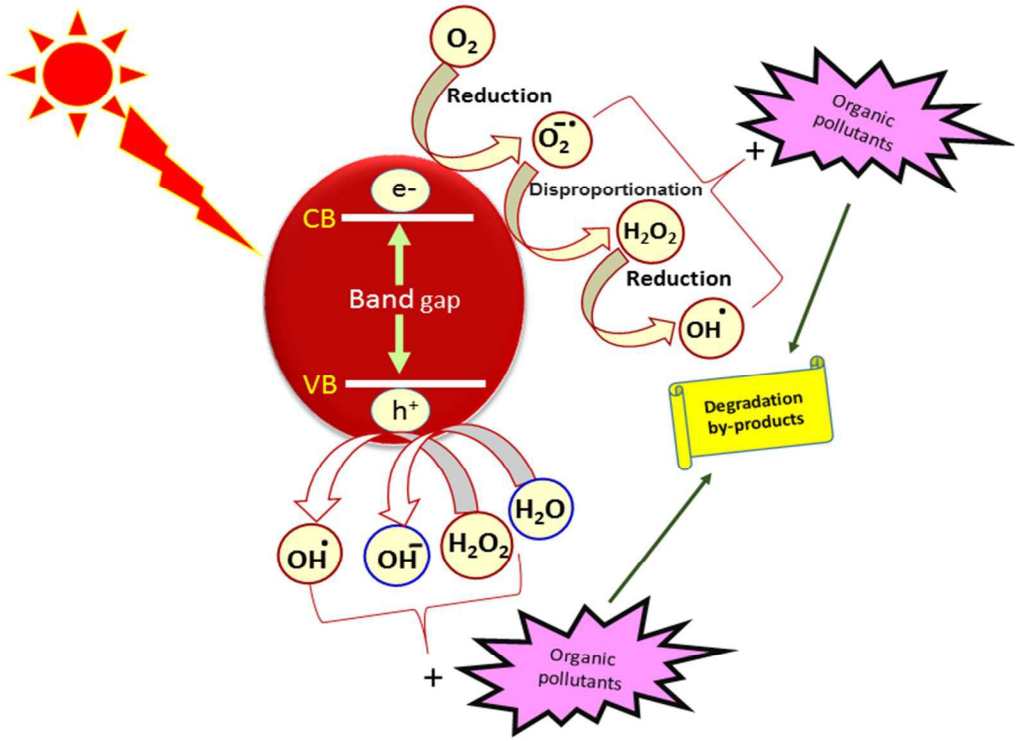

Fig.2 Schematic illustration of a semiconductor particle based photocatalyst for organic pollutant degradation.

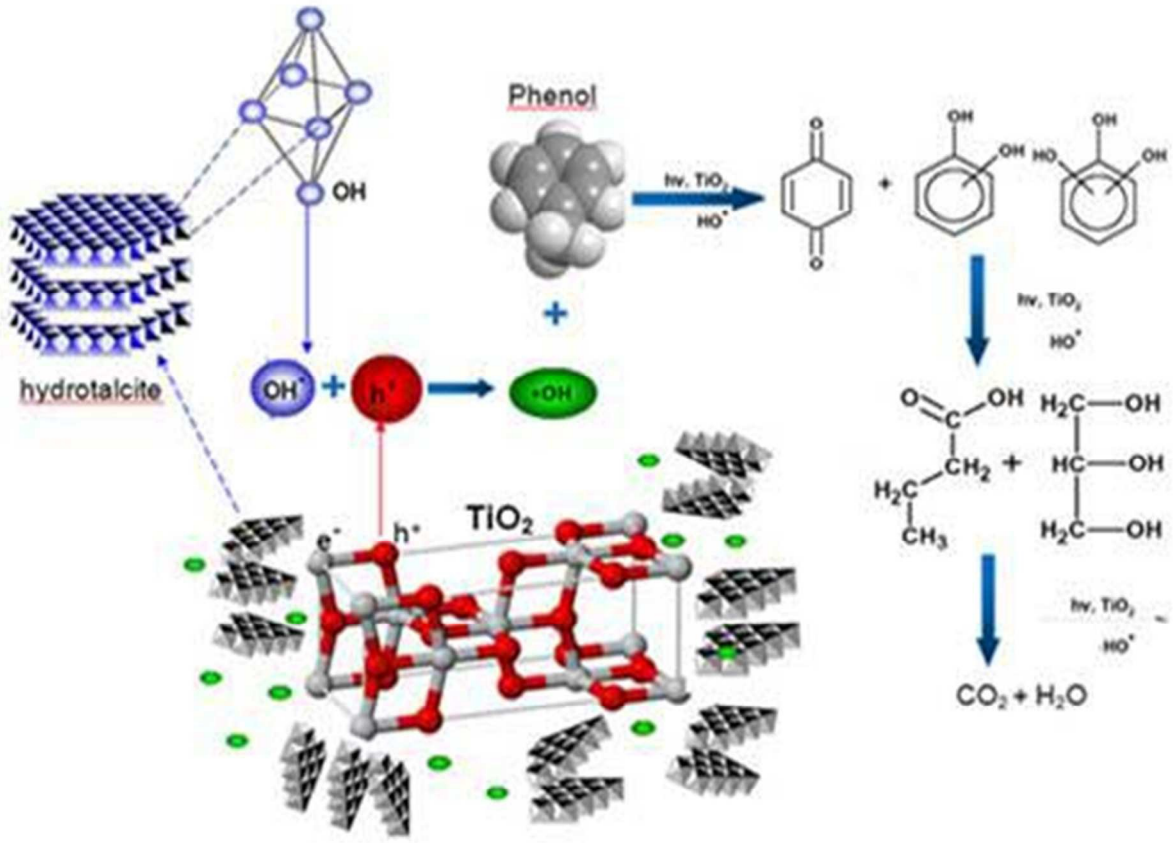

Fig. 3 Proposed mechanism for the photocatalytic degradation of phenol in presence of a mixture of TiO_2 /Mg–Al layered double hydroxides (adapted with permission from ref. 59 @ copyright 2011 Elsevier).

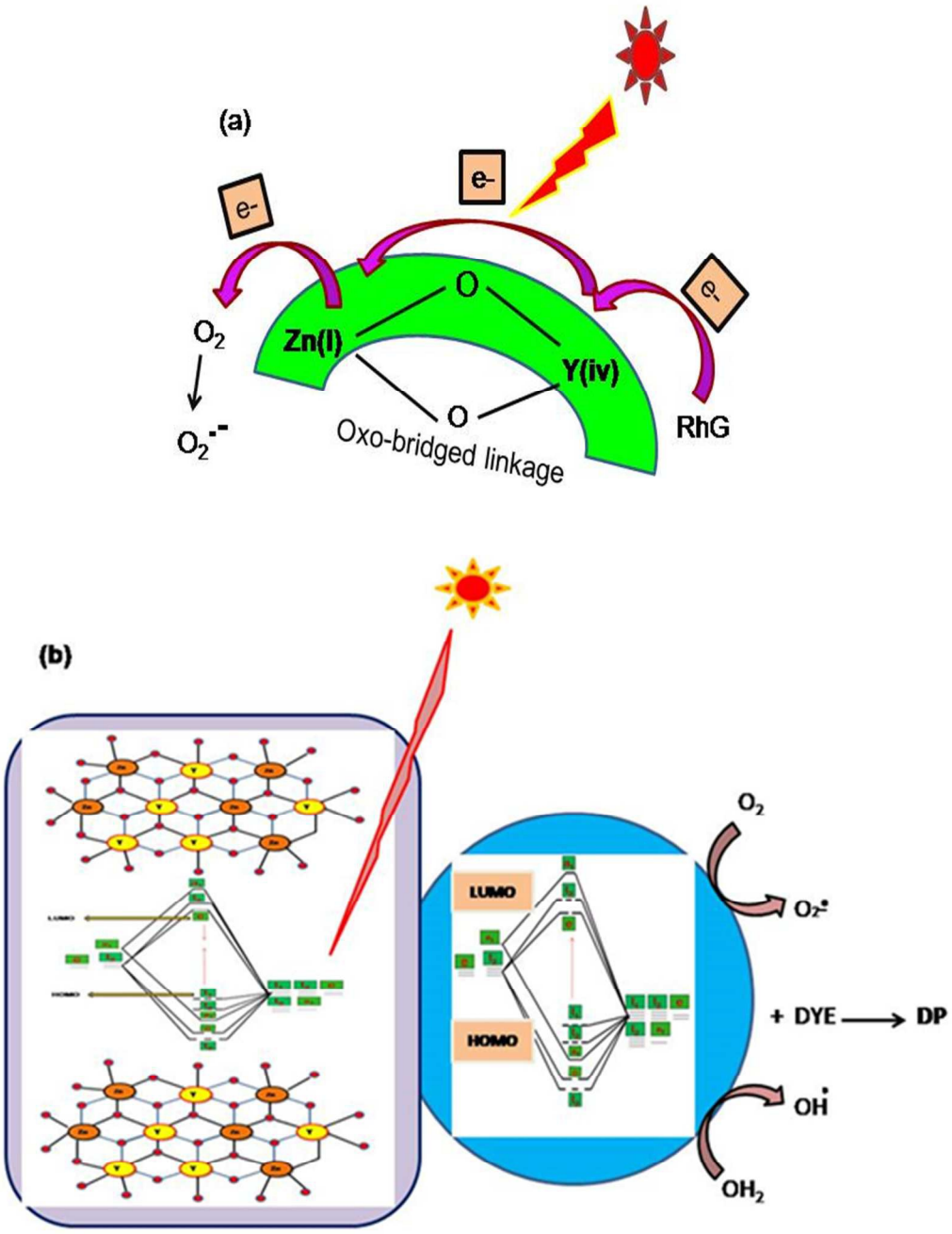

Fig.4 (a) Schematic illustration of anchored Zn(II)/Y(III) bimetallicoxo-linkage on the Zn/Y LDH and its photocatalysis driven by the photoinduced MMCT,(b)Schematic illustration of the photocatalysis occurring on the Zn/Y/M LDH under visible light irradiation. HOMO and LUMO of intercalated

molybdate and tungstate in Zn/YLDH and DP is the dye product ('a, b' from ref. 29 @ 2012 American Chemical Society).

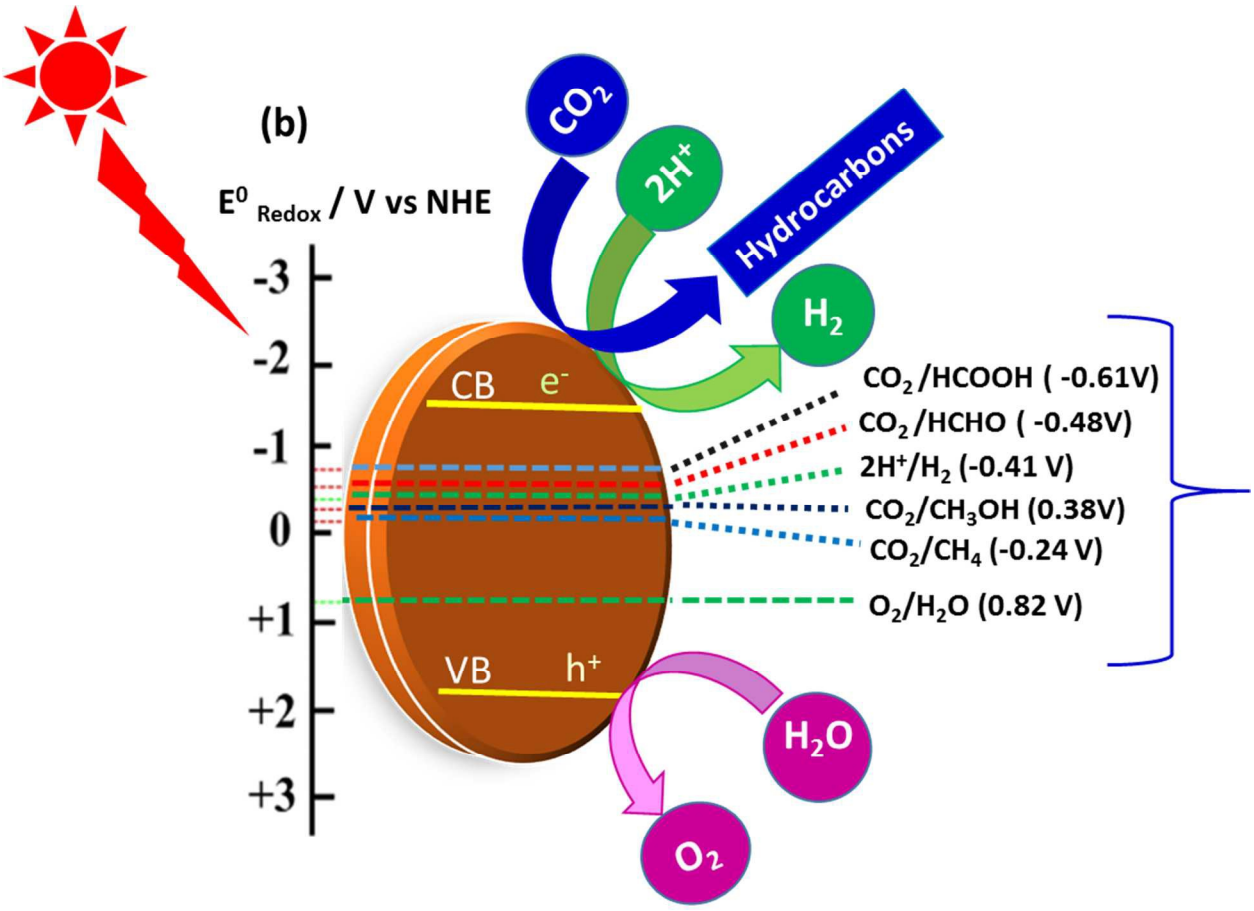

Fig. 5 Schematic energy diagrams of the semiconductor for photocatalytic water splitting and CO_2 reduction process (redox potentials are converted to NHE reference, pH = 7).

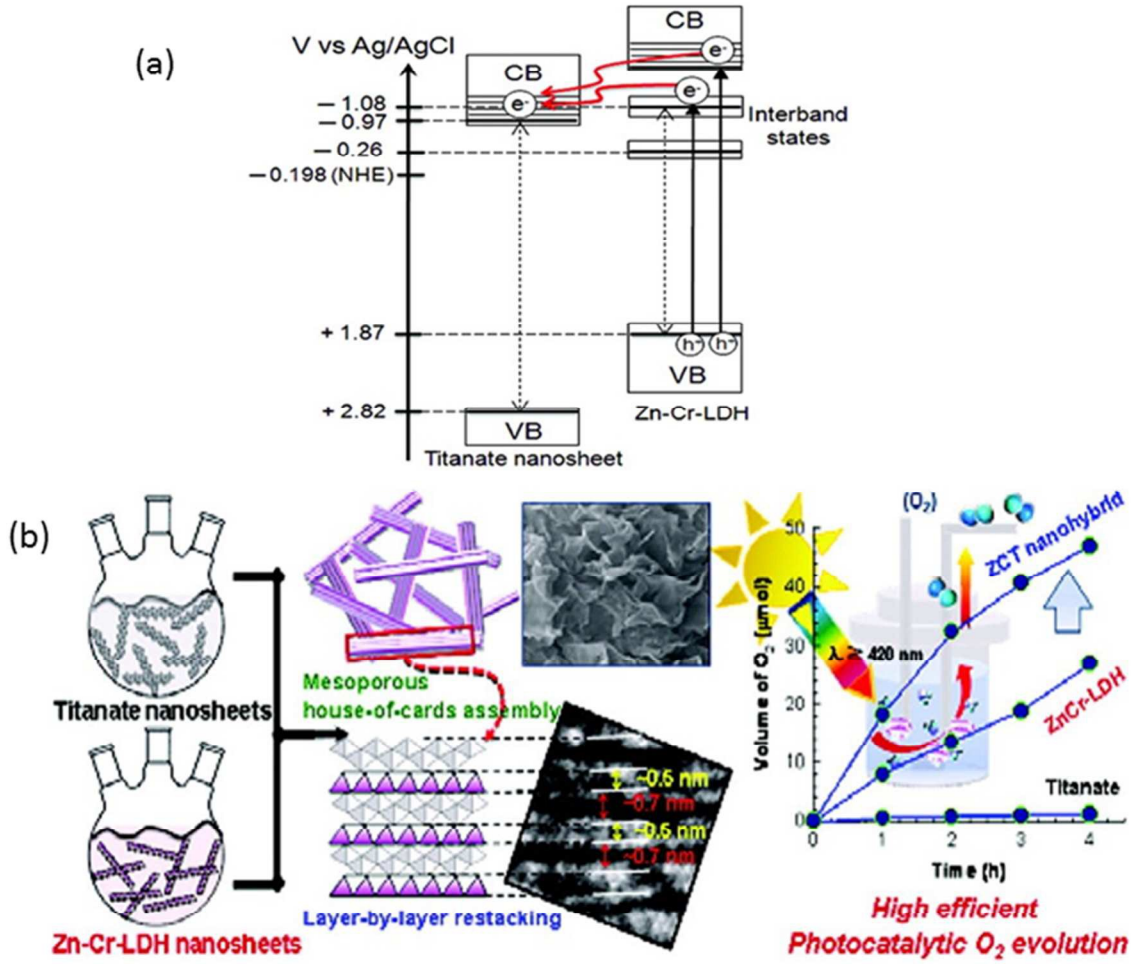

Fig. 6 (a) Band structure of layered titanate/Zn-Cr-LDH nanohybrid (b) Total mechanism and activities for O_2 evolution(ref. 41 @ 2011 American Chemical Society).

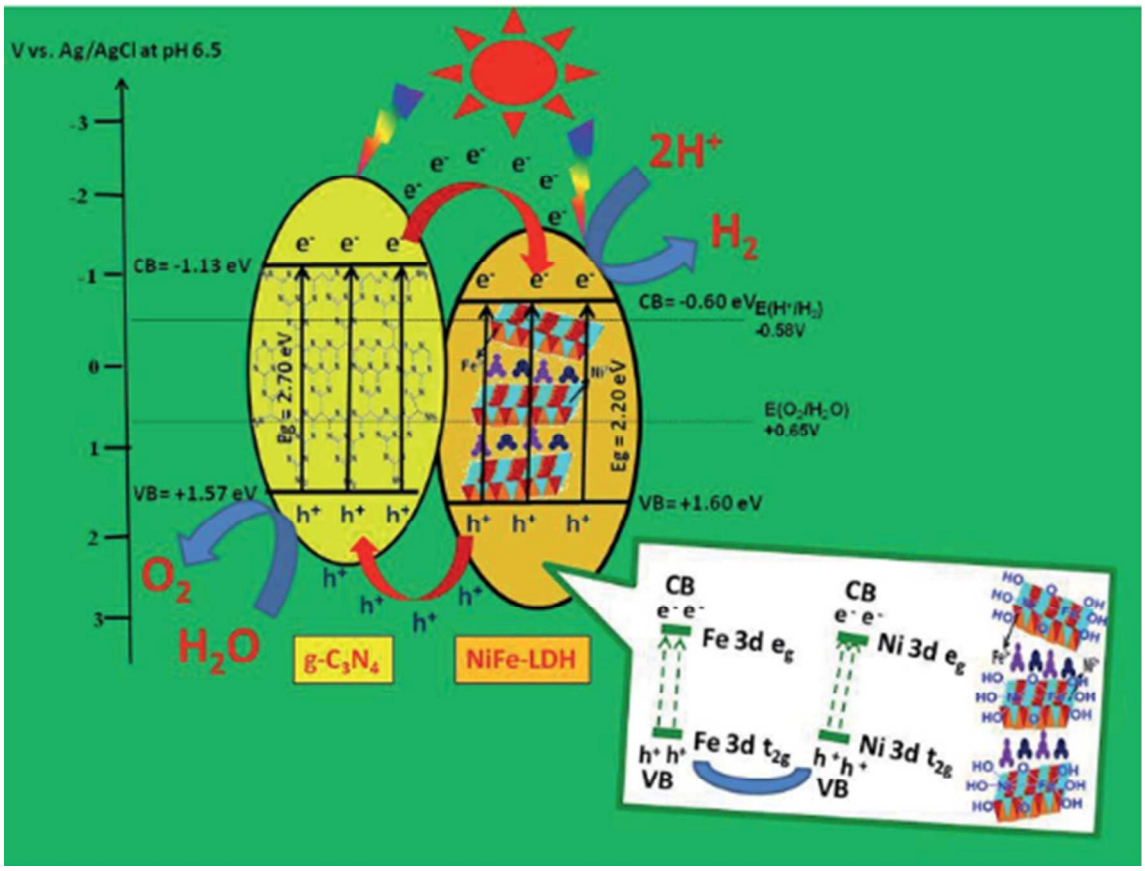

Fig. 7 Mechanistic scheme for evolution of hydrogen and oxygen under visible-light irradiation by Ni-Fe LDH/g-C3N4 composite materials. (ref. 135 @ 2013 Royal Chemical Society).

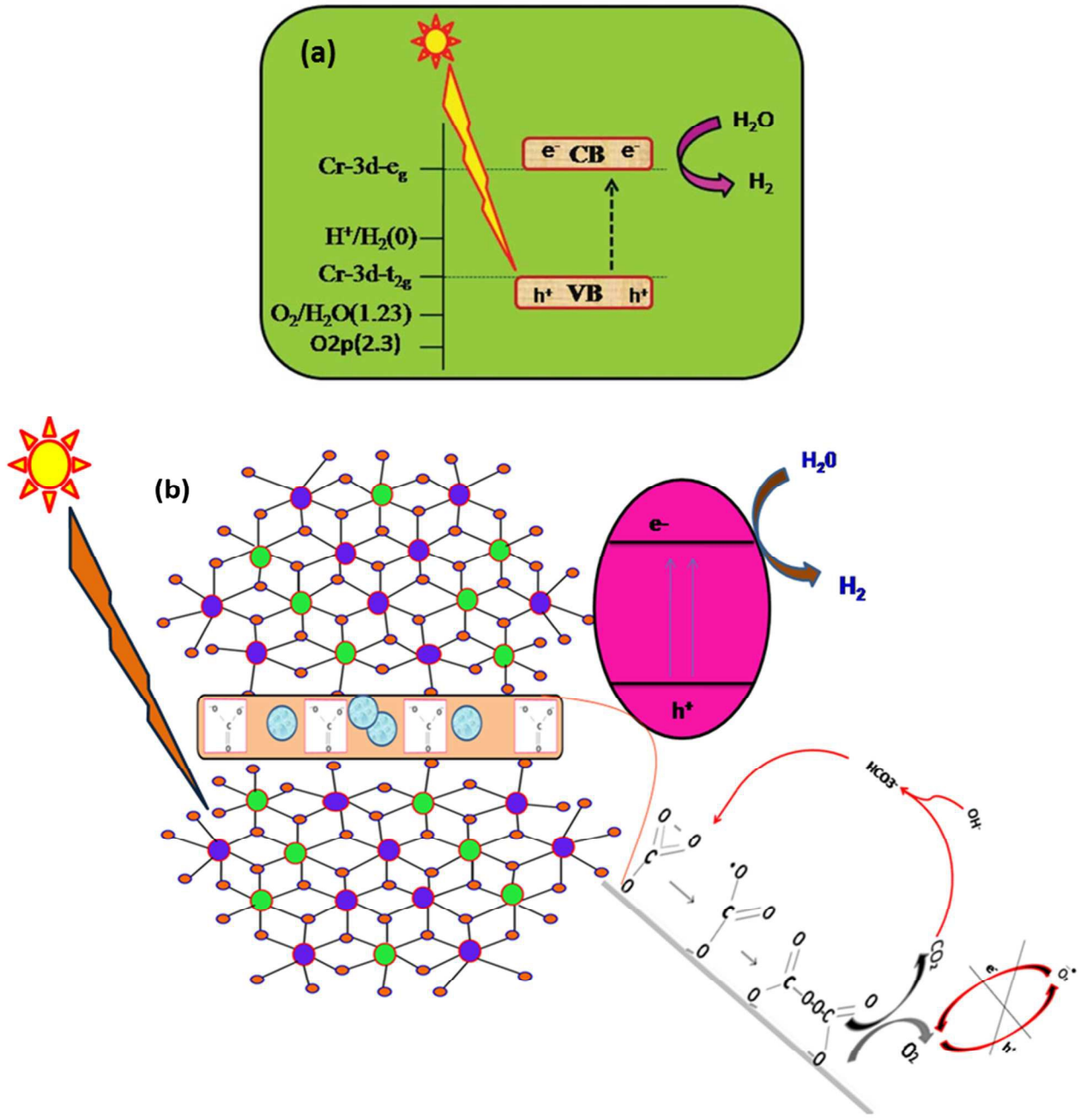

Fig.8 (a) The proposed reaction scheme for photo-excition of electrons from Cr-3dt_{2g} to Cr-3d$_{eg}$ on CrO_6 octahedron of Zn/Cr LDH by irradiation of visible light (b) The mechanism of enhanced photocatalytic hydrogen evolution of carbonate intercalated Zn/Cr LDH under visible light irradiation (ref. 26 @ 2012 Royal Chemical Society).

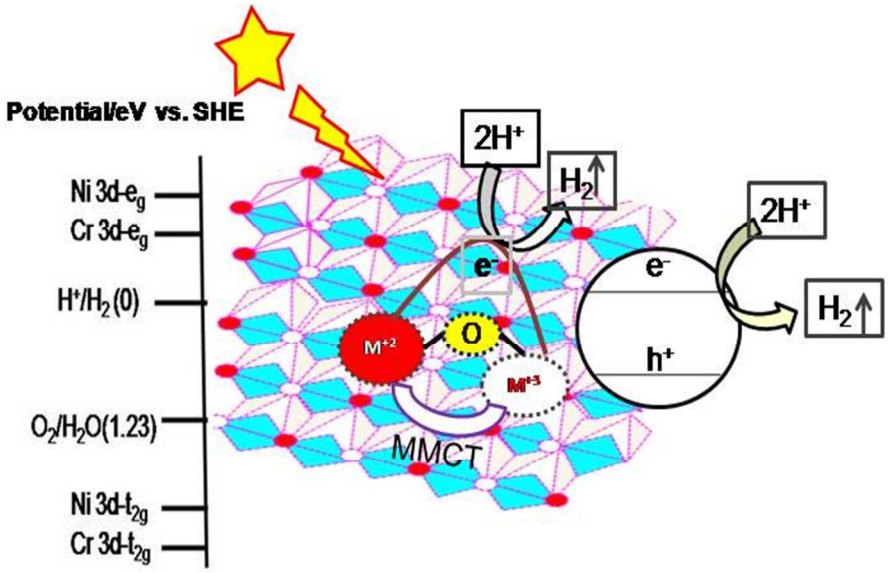

Fig. 9. Schematic representation of the total mechanism for hydrogen evolution over Ni+Zn/Cr LDH under visible light irradiation (ref. 36 @ 2013 Royal Chemical Society).

Table 1. Summary of LDH photocatalysts for degradation of organic pollutants.

LDH based photocatalyst	Pollutant type	Light source/Incident Light	Degradation activities of photocatalyst	Time	Reference
Mg/Al LDH	2-Chlorophenol	Intensity of 4400 $\mu W/cm^2$ and λ ~ 254 nm	rate ~ 95%	4 h	81
Zn/Fe-Cl LDH Zn/Fe-NO_3 Zn/Fe-CO_3	Methyl violet, Malachite green Methyl violet, Malachite green Methyl violet, Malachite green	Exposed to solar light and the average light intensity was 10,4000 Lx	Rate ~ 75%, 72% rate~ 66%, 64% rate ~ 99%	2h 2h 2h	29
Zn/Ti (3:1) LDH	methylene blue	300 W Xe, λ = 420 nm	rate ~ 96%	2 h	22
C–N–TiO_2	Methylene blue	300 W high-pressure mercury lamp	rate ~ 50% (visible light irradiation) rate ~ 100% (UV light irradiation)	3 h	97
Ni/Ti (2:1) LDH NiO	Methylene blue	300 W tungsten lamp as the visible-light source, equipped with a wavelength filter (λ > 400 nm)	rate ~99.8% rate ~ 83%	1.25 h	99
Co/Ti (2:1) LDH CoO	Congo-Red	300 W tungsten lamp as the visible-light source, equipped with a wavelength filter (λ > 400 nm)	rate ~ 99.7% rate ~ 82%	1.25 h	100
Zn/Cr LDH	Xanthene dyes 4-chloro 2-nitro phenol	Exposed to solar light and the average light intensity was 10,4000 Lx	rate ~ 95%	2 h	26
M-Cr/NO_3 LDHs (M=Cu,Ni,Zn)	Congo-Red	300 W Xe , λ > 400 nm	rate ~ 80%	1.5 h	66
Cu/Cr-LDH film	2,4,6-TCP SRB Congo red	300 W Xe , λ > 400 nm	rate ~ 88% rate ~ 97%	1.6h	102

M^{II} /Cr ^{III} CO_3 LDH	Methyl orange	Exposed to solar light and the average light intensity was about 104,100 Lx	rate ~ 90%	3h	103
Cu+Co/Cr LDH	Malachite green	Exposed to solar light and the average light intensity was about 104 ,100 Lx	rate ~ 99%	4h	35
$Zn^{2+}/Al^{3+}+Fe^{3+}$ LDH	phenol and p-cresol	Intensity of 4400 $\mu W/cm^2$ and λ ~ 254 nm	rate ~ 98%	6h 4 h	106
Zn-Bi LDH	Malachite green Rhodamine 6G 4-chloro,2-nitrophenol	Exposed to solar light and the average light intensity was around 10, 5000 Lx	rate ~ 65 % rate ~ 62 % rate ~ 58 %	3h	127
Mg/Zn–In LDH Calcined Mg/Zn–In LDH	methylene blue methylene blue	300 W Xe , λ = 420nm	rate ~ 90% rate ~ 97%	1.67h 1.67h	109 109
Mg-Al-Zn Mixed-oxide	C. I. Basic Blue	UV-C irradiation source 15 W Xe , λ = 254 nm	rate ~ 98%	4h	111
Zn Al In-MMO	methylene blue	300 W Xe , λ = 420nm	rate ~ 73	4h	112
MgO/ZnO/In_2O_3 MMO	methylene blue	300 W Xe , λ = 420nm	rate ~ 98%	5h	113
TiO_2/Mg-Al LDH	Phenol	Fluorescent black light tube UV Philips, 8 W, λ=365 nm	rate ~ 99%	8 h	39
TiO_2/Zn LDH	Phenol	Intensity of 4400 $\mu W/cm^2$ and λ ~ 254 nm	rate ~85%	4 h	38
CeO_2/Mg-Al LDH	Phenol	Intensity of 4400 $\mu W/cm^2$ λ== 254 nm	rate ~ 50 %	7 h	39
SnO_2/Mg-Al LDH	Methelene blue	6 W Vilber Lourmat UV-lamp, λ== 254 nm	rate ~ 97%	1h	30
Biotemplated Zn/Al-MMO	Sulfo-rhodamine B Azo benzene dye	UV light produced from mercury lamp.	rate ~ 81% rate ~ 74%	2h 2h	117
Zn/Al-LDH/CNTs	Methyl orange	The UV light was irradiated from two 36	rate ~ 93%	7 h	118

		W H-type lamps, λ= 254 nm			
Fe_3O_4/Zn-Cr-LDH	Methelene blue	300 W Xe , λ ≥ 420nm	rate ~ 95%	3 h	120
Bi_2MoO_6/Zn–Al LDH	Rhodamine G	400 W Xe , λ ≥ 420nm	rate ~ 99%	80min	121
Ag_3PO_4/FLDH	Acid red G	400 W Xe , λ ≤ 420nm	rate ~ 95%	1 h	123
Ni/Mg Al LDH Ni/MgFe Al LDH	drimaren red drimaren navy drimaren red drimaren navy	Intensity of 4400 μW/cm^2 and λ ~ 254 nm	Rate ~ 70% rate ~ 70% Rate ~ 84% rate ~ 80%	6h 6h 6h 6h	124
rCG/ZnAl-LDO	Methelene blue	300 W Xe , λ = 420nm	rate ~ 100%	2h	126
Ag/AgBr/Co-Ni LDH	Methyl orange	300 W Xe , λ = 400nm	rate ~ 100 %	2 h	48
Zn-Bi/ Decavanadate LDH	Malachite green Rhodamine 6G 4-chloro,2-nitrophenol	Exposed to solar light and the average light intensity was around 10, 5000 Lx	rate ~ 90% rate ~ 87% rate ~ 85%	1h	127
Zn/Y-MoO_4 LDH Zn/Y-WO4 LDH	Rhodamine 6G Rhodamine 6G	Exposed on whole range of Solar light	rate ~ 98% rate ~ 84%	2 h 2h	29 29
Zn_3Al–CuPc LDH	Methelene blue	Exposed on whole range of Solar light	rate ~ 75%	4h	128

Graphical abstract

A Review on Recent Progress, Challenges and Perspective of Layered Double Hydroxides as Promising Photocatalysts

Lagnamayee Mohapatra * [a] and K. M. Parida ** [b]

[a] Centre for Advanced Materials, Qatar University, P.O. Box 2713, Doha, Qatar

[b] Centre for Nano Science and Nano Technology, ITER, Siksha 'O'Anusandhan University

Bhubaneswar-751 030, Odisha (India)

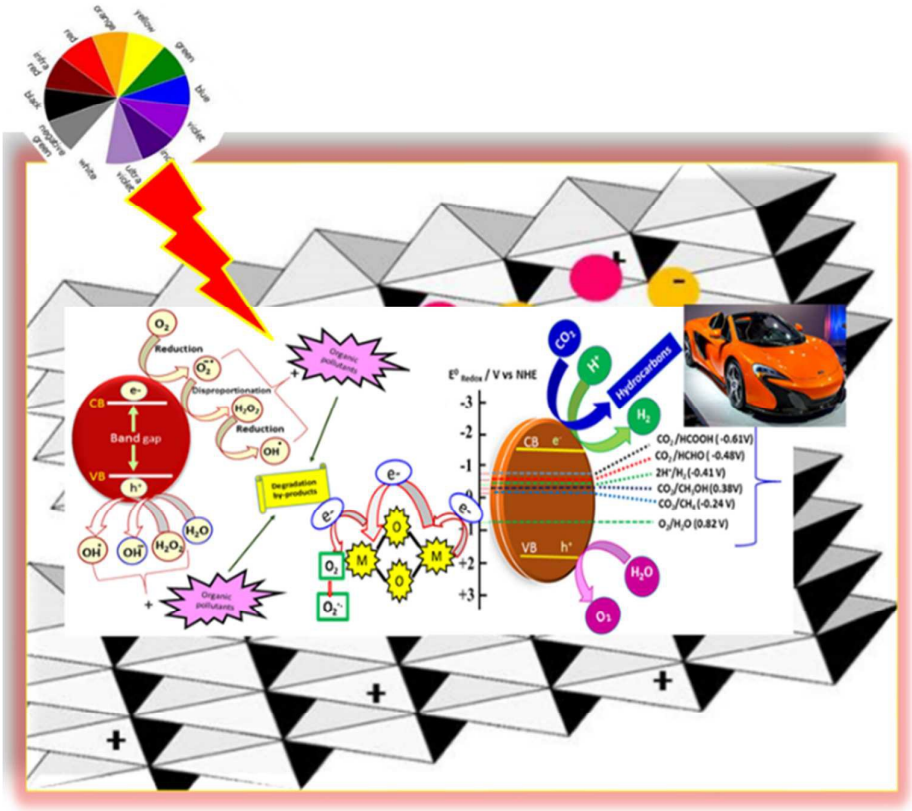

The present review article evaluates the effectiveness and special features of LDH/modified LDH on the photocatalytic activities.